A DYNAMIC MODEL OF THE HUMAN/COOLING SYSTEM/CLOTHING/ENVIRONMENT SYSTEM

by

ZHENGXIANG PU
B.E. Xi'an Jiaotong University, 1996
M.S. Xi'an Jiaotong University, 1999

A dissertation submitted in partial fulfillment of the requirements
for the degree of Doctor of Philosophy
in the Department of Mechanical, Materials and Aerospace Engineering
in the College of Engineering and Computer Science
at the University of Central Florida
Orlando, Florida

Spring Term
2005

Major Professor: Jayanta S. Kapat
Louis C. Chow

ABSTRACT

The human body compensates well for moderate climatic heat stress, but artificial environments often block or overwhelm physiological defense mechanism. Personal protective equipment (PPE) is one of sources of heat stress. It protects individual from chemical, physical, or biological hazards, but the high thermal insulation and low vapor permeability of PPE may also lead to substantial heat stress. Personal cooling is widely used to alleviate heat stress, especially for those situations where ambient environmental cooling is not economically viable or feasible.

It is important to predict the physiological responses of a person wearing PPE with personal cooling to make sure that the individual is free of heat stress, as well as any additional discomfort that may occur. Air temperature, radiant temperature, humidity and air movement are the four basic environmental parameters that affect human response to thermal environments. Combined with the personal parameters of metabolic heat generated by human activity and clothing worn by a person, they provide the six fundamental factors which define human thermal environments. If personal cooling system is available, the fluid flow speed, cooling tube distribution density and fluid inlet temperature have significant effects on the human thermal comfort. It is impractical to evaluate the problem experimentally due to too many factors involved.

A thermal model was developed to improve human body thermal comfort prediction. The system researched includes human body, personal cooling system, clothing and

environment. An existing model of thermoregulation is taken as a starting point. Changes and additions are made to provide better prediction. Personal cooling model was developed and it includes liquid cooling model, air cooling model and ice cooling model. Thermal resistance networks for the cooling system are built up; additionally a combined model of heat and mass transfer from cooling garment through clothing to environment is developed and incorporated into the personal cooling model and thermoregulatory model. The control volume method is employed to carry out the numerical calculation. An example simulation is presented for extra-vehicular activities on Mars.

The simulation results agree well with available experimental data, though a small discrepancy between simulation results and experimental data is observed during the beginning of the cooling process. Compared with a water cooling lumped model, the thermal model provides a much better prediction. For water cooling, parametric study shows that the cooling water inlet temperature and liner thermal resistance have great effects on the maximum exposure time; PPE resistance and cooling water flow rate do not have much impact on the maximum exposure time. For air cooling, cooling air flow rate, inlet temperature, relative humidity and liner resistance have great effects on the maximum exposure time.

I would like to dedicate this dissertation to my wonderful family. Particularly to my understanding and patient wife, Yan, who has put up with these many years of research, and to our precious daughter Rachel, who is the joy of our lives. I must also thank my loving parents and my terrific in-laws who have helped so much with baby-sitting and have given me their fullest support.

ACKNOWLEDGMENTS

I would like to thank all of those people who helped make this dissertation possible.

I would like to express my deepest gratitude and thankfulness to my advisor Dr. Jay Kapat and co-advisor Dr. Louis Chow for all their guidance, encouragement, support, and patience. Their sincere interests in science have been a great inspiration to me. Also, I would like to thank my committee members Dr. Ruey-Hung Chen, Dr. Gene Lee and Dr. Xin Li for their very helpful insights, comments and suggestions. Additionally, I would like to acknowledge Dr. Thomas Bernard from the University of South Florida, for his great support and help regarding to the research.

Finally, I would like to thank the excellent faculty, staff and students at the Material, Mechanical and Aerospace Engineering Department of the University of Central Florida. Particularly, I would like to thank Dr. Alan Kassab, Dr. Antonio Minardi, Dr. Quanfang Chen and Dr. David Nicholson, for their guidance and help in my study.

TABLE OF CONTENTS

LIST OF FIGURES

LIST OF TABLES

LIST OF NOMENCLATURE

A	Heat transfer area, m^2
A_D	Surface area of human body, m^2
A_{eff}	Effective radiation area of the clothes body , m^2
$BF(N)$	Blood flow rate for compartment N
$BFB(N)$	Basal blood flow rate for compartment N
$C(N)$	Heat capacity for compartment N
$C_{ST}(N)$	Heat capacity for compartment N for standard man
C_{res}	Sensible respiration heat loss, W
$COLD$	Output from cold receptors in compartment
$COLDS$	Integrated output from skin cold receptors
E	Evaporative heat loss
E_{res}	Latent respiration heat loss, W
E_{max}	Maximum evaporation heat loss, W
$ERROR$	Output from thermo-receptors
f_c	Clothing surface area correction factor
f_{eff}	Effective radiation area factor
h_c	Convective heat transfer coefficient
h_e	Evaporative heat transfer coefficient on the skin
$Height$	Height of human body, cm
k_{skin}	Thermal conductivity of the skin, W/(m·°C)

$k_{skin\text{-}fat}$	Thermal conductivity between skin layer and fat layer
M	Metabolic rate
N_u	Nusselt number
O_e	Fraction of oxygen in expired air
O_i	Fraction oxygen in inspired air
P_a	Partial pressure of water vapor in environment
P_{mem}	Partial pressure of water vapor in the microenvironment
P_{in}	Partial pressure of water vapor in inspired air, mb
P_r	Prandl number
P_{skin}, P_s	Partial pressure of water vapor on skin
PPE	Personal protective ensembles
Q	Heat, W
R	Heat resistance
R_e	Renolds number
RH	Relative humidity
r_{fat}	Radius of fat layer, m
r_{skin}	Radius of body part, m
T	Temperature, °C
T_a	Ambient temperature, environment temperature, °C
T_{cl}	Temerpature of clothing, °C
T_{db}	Dry bulb temperature, °C

T_{in}	Inspired air temperature, °C
T_m	Mean radiant temperature, °C
T_s	Skin temperature, °C
T_{wb}	Wet bulb temperature, °C
V	Ventilation rate
v	Air velocity, m/s
v_{eff}	Effective air velocity, m/s
W	External work, W
$WBGT$	Wet bulb global temperature, °C
$Weight$	Mass of human body, kg
ΔT	Temperature difference, °C
Δt	Time step
Δx	Distance between two adjacent nodes
Δx_w	Distance between two adjacent nodes beneath water nodes
α	Solar absorptance
ε	Infrared emittance (=absorptance) of the outer suit material
η	Mechanical efficiency
ρ	Density, kg/m^3
λ	Overall conductance of clothing, W/m^{2}K
σ	Stephen- Boltzmann constant
μ	Dynamic viscosity, P_a s

Definitions Of Symbols Used In Description Of The Controlling System In The Thermoregulatory Model

TSET(N)	Set temperature or reference point for receptors in compartment N, °C
ERROR(N)	Output from thermo-receptors in compartment N, °C
RATE(N)	Dynamic sensitivity of thermo-receptors in compartment N, °C
COLD(N)	Output from cold receptors in compartment N, °C
WARM(N)	Output from warm receptors in compartment N, °C
COLDS	Integrated output from skin cold receptors, °C
WARMS	Integrated output from skin warm receptors, °C
SWEAT	Total efferent sweat command, W
CHILL	Total efferent shivering command, W
DILAT	Total efferent skin vasodilatation command, l/hr
STRIC	Total efferent skin vasoconstriction command
SKINR(I)	Fraction of all skin receptors in segment I
SKINS(I)	Fraction of sweating command applicable to skin of segment I
SKINV(I)	Fraction of vasodilatation command applicable to skin of segment I
SKINC(I)	Fraction of vasoconstriction command applicable to skin of segment I
WORKM (I)	Fraction of total work done by muscles in segment I
CHILM (I)	Fraction of total shivering occurring in muscles in segment I

Definitions Of Symbols Used As Control Coefficients In Thermoregulatory Model

CSW	Sweating from head core, $W/°C$

SSW	Sweating from skin, $W/°C$
$CDIL$	Vasodilatation from head core, $l/(hr \cdot °C)$
$SDIL$	Vasodilatation from skin, $l/(hr \cdot °C)$
$CCON$	Vasoconstriction from head core, $°C^{-1}$
$SCON$	Vasoconstriction from skin, $°C^{-1}$
$CCHIL$	Shivering from head core, $W/°C$
$SCHIL$	Shivering from skin, $W/°C$
PSW	Sweating from skin and head core, $W/°C^2$
$PDIL$	Vasodilatation from skin and head core, $l/(hr \cdot °C^2)$
$PCON$	Vasoconstriction from skin and head core, $°C^{-2}$
$PCHIL$	Shivering from skin and head core, $°C^{-2}$
$BULL$	Factor determining temperature sensitivity of sweat gland response $°C^{-1}$

CHAPTER 1 INTRODUCTION

The aim of this dissertation is to develop a thermal model to predict human response to environment. Such prediction becomes more difficult when personal protective ensembles (PPE) and personal cooling system are integrated in the system. This chapter introduces thermal regulation of human body and basic information of PPE and personal cooling system.

Personal Protective Ensembles

Personal protective equipment, or PPE, is designed to protect individuals from chemical, physical, and biological hazards that may be encountered during hazardous materials operations. Personal protective ensembles are required when the working environment poses a threat to the wearer's health. Situations in which they are necessary include soldiers in nuclear/biological/chemical war, cleaners in a nuclear plant, astronauts in space, etc. Besides face shields, safety glasses, hard hats, and safety shoes, PPE includes a variety of devices and garments such as coveralls, gloves, vests, earplugs, and respirators.

There are basically four levels of personal protective equipment: Level A protection is required when the greatest potential for exposure to hazards exists, and when the greatest level of skin, respiratory, and eye protection is required. Examples of Level A clothing and equipment include positive-pressure, full face-piece self contained breathing apparatus (SCBA) or positive pressure supplied air respirator with escape SCBA, totally encapsulated chemical- and vapor-protective suit, inner and outer chemical-resistant gloves, and disposable protective suit, gloves, and boots.

Level B protection is required under circumstances requiring the highest level of respiratory protection, with lesser level of skin protection. At most abandoned outdoor hazardous waste sites, ambient atmospheric vapors or gas levels have not approached sufficiently high concentrations to warrant level A protection -- Level B protection is often adequate. Examples of Level B protection include positive-pressure, full face-piece self contained breathing apparatus (SCBA) or positive pressure supplied air respirator with escape SCBA, inner and outer chemical-resistant gloves, face shield, hooded chemical resistant clothing, coveralls, and outer chemical-resistant boots.

Level C protection is required when the concentration and type of airborne substances is known and the criterion for using air purifying respirators is met. Typical Level C equipment includes full-face air purifying respirators, inner and outer chemical-resistant gloves, hard hat, escape mask, and disposable chemical-resistant outer boots. The difference between Level C and Level B protection is the type of equipment used to

protect the respiratory system, assuming the same type of chemical-resistant clothing is used. The main criterion for Level C is that atmospheric concentrations and other selection criteria permit wearing an air-purifying respirator.

Level D protection is the minimum protection required. Level D protection may be sufficient when no contaminants are present or work operations preclude splashes, immersion, or the potential for unexpected inhalation or contact with hazardous levels of chemicals. Appropriate Level D protective equipment may include gloves, coveralls, safety glasses, face shield, and chemical-resistant, steel-toe boots or shoes.

When any material, such as personal protective equipment covers the body, a microenvironment is formed between the clothing and the skin. Generally, this microenvironment quickly becomes warmer and more humid than ambient environment because of the production of metabolic heat and sweat by person. Protective suits usually contain multiple layers with different functions, including thermal barrier, vapor/water barrier, flame resistant and so on. Thermal barrier, which usually has high thermal insulation value and low vapor permeability, limits heat loss from the body. Furthermore, if the PPE is vapor impermeable, the microenvironment gets even worse because the sweat evaporation is also prevented. This produces a significant health risk because the lack of heat loss from the body could lead to suffering from discomfort and heat stress.

Thermal Regulation of Human Body Comfort and Heat Stress

The human body, being warm blooded, is functional only when body temperature is maintained within a very narrow range. The complex reactions that convert food, water and oxygen into the chemical and electrical energies that power and sustain life are extremely temperature dependent. This “core” temperature normally varies from 36°C to 38°C. If the core temperature goes up or down by just a few degrees, those reactions no longer occur in a normal manner and human body will be in a life-threatening situation. Heat stress is assumed to occur when the trunk core temperature reaches 38.5ºC in this dissertation. Human body maximum exposure time is the time when the trunk core temperature reaches 38.5ºC.

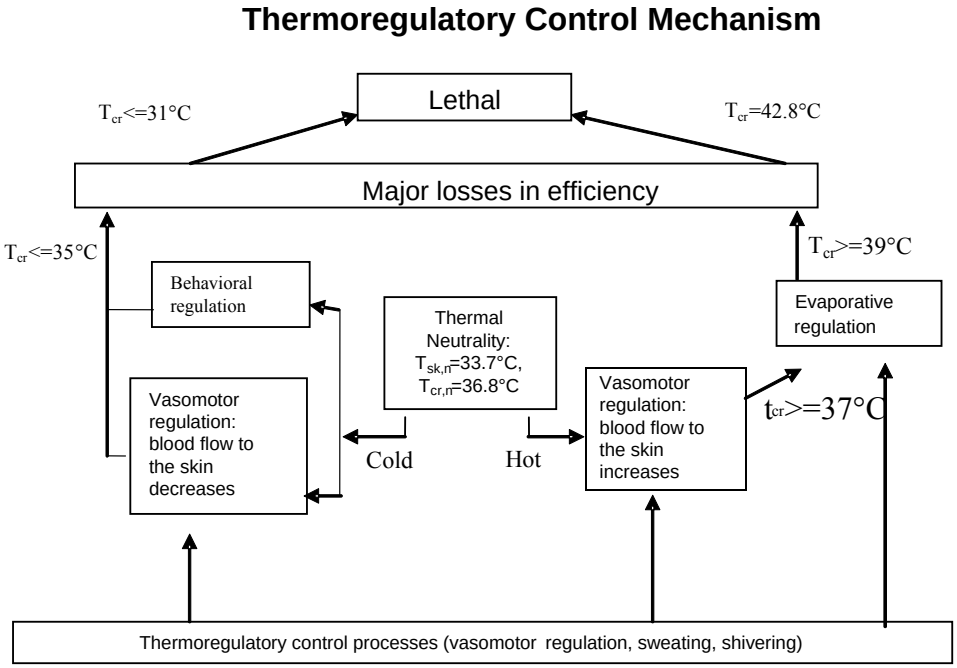

Figure 1.1 Human Body’s Reactions to Thermal Environment with Thermoregulatory Behaviors.

A person performing heavy work in a hot environment builds up body heat quickly. To keep internal body temperatures within safe limits, the body must get rid of its excess heat, primarily through varying the rate and amount of blood circulation through the skin and the release of fluid onto the skin by the sweat glands. In this process of lowering internal body temperature, the heart begins to pump more blood, blood vessels expand to accommodate the increased flow, and the microscopic blood vessels (capillaries) which thread through the upper layers of the skin begin to fill with blood. The blood circulates closer to the surface of the skin, and the excess heat is lost to the cooler environment. Figure 1.1 schematically shows human body's reactions to thermal environment with thermoregulatory behaviors.

Thermal comfort is defined as the condition of mind that expresses satisfaction with the thermal environment (ASHRAE 1992). From the physiological point of view, thermal comfort occurs when there is a thermal equilibrium in the absence of regulatory sweating between the human body and the environment. Factors influencing thermal comfort include temperature, humidity, air movement, radiant temperature of surroundings, a person's clothing and physical activity.

Excessive exposure to a hot work environment can bring about a variety of heat stress. The effects of heat stress range from simple discomfort to life threatening illnesses such as heat stroke. Heat stroke is the most serious of health problems associated with

working in hot environments. It occurs when the body's temperature regulatory system fails and sweating becomes inadequate.

Mechanism of Heat Dissipation to the Environment

When heat is transferred from the core to the skin, several mechanisms are employed to lose the heat to the environment. The most important of these mechanisms are evaporation, convection and radiation.

Evaporation

Sweating is the body’s most effective mechanism for losing heat in a hot and/or heavy work environment because of the large heat of vaporization of water. Evaporative heat loss could occur even when surrounded by a temperature higher than body temperature. Heat loss at a rate of 2.43 KJ per gram of evaporated sweat occurs as heat from the skin is used to evaporate the sweat. The average person has 2.6 million sweat glands. Sweat is made up of water and electrolytes such as sodium, chloride, and potassium. When the hypothalamus senses an increase in core temperature it will act by increasing blood flow to the skin, stimulating the sweat glands. The result is an increase in the rate of water lost through sweating. The maximum sweat rate that can be maintained by a healthy, well-acclimatized young male is about 2 liter per hour. Even when one is unaware of sweating, an amount of about 600 grams per day of "insensate loss" of moisture evaporates from the skin. To be effective in cooling the body, the sweat must

actually evaporate from the skin instead of dripping off or being wiped off. The rate of evaporation depends upon ambient temperature and relative humidity. For human body wearing PPE, especially level A PPE, Evaporation can not provide effective cooling because PPE forms a microenvironment with high humidity which prevents the sweat evaporating on the human skin.

Convection

Convection results from the movement of air over the body. Whenever air that is cooler than the body is blown across the body surface, then heat can be removed from the skin surface. The rate of heat loss by convection depends upon factors such as air temperature, wind speed and type of clothing. If the air is actually hotter than the skin, a reverse transfer of heat from the air to the body will occur.

Radiation

The body continually loses heat via electromagnetic waves whenever the body temperature is warmer than the surrounding environment. Skin that has been warmed by blood flow from the core radiates heat to the surrounding environment. If the environment includes surfaces or systems such as furnaces or boilers that are significantly hotter than the skin, the flow of heat by radiation may also reverse and go from the environment to the body, thereby adding to the total heat load of the body. The rate of heat transfer by radiation is a function of the types of surfaces involved and the

temperature difference between them. The direction of radiant heat flow is always from a warmer surface to a cooler surface.

Convection and radiation heat transfer could not remove the heat from PPE wearers' body directly. The heat has to be transferred from microenvironment to PPE by conduction first, and then the heat is removed from PPE outside surface by convection and radiation. Since most personal protective equipments include a layer of thermal barrier, which has high thermal insulation value, it makes the heat transfer from microenvironment to PPE outside surface very ineffective. It is concluded that both convection and radiation could not remove heat from human body effectively.

Personal Cooling System

Personal cooling is one widely used way to alleviate heat stress. It can be divided into two major categories, passive and active, the latter having moving parts and requiring attachment to an energy source. Ice, cooled liquid and cooled air are the most often medium used to remove excess heat from the human body in a personal cooling system.

Phase change of water or another substance can be used for passive cooling. Ice vest is a garment which contains pockets of frozen water. The ice vest cools the microclimate through melting the ice and warming the result water. The very low starting

temperature of the heat sink means that the vest must be worn over an insulation garment to prevent skin chilling. Ice vest is easy and economical to use. However, its application is limited to moderate temperature environment and where only short term cooling is needed.

Active systems use an external heat sink to cool a fluid, usually air or water, which is then pumped through the clothing system to provide microclimate conditioning. The heat picked up by the cooling loop may come from metabolism and from the environment. External heat sinks can be based on many different mechanisms. Sweating does not cool the body unless the moisture is removed from the skin by evaporation. Under conditions of high humidity, the evaporation of sweat from the skin is decreased and the body's efforts to maintain an acceptable body temperature may be significantly impaired. In a personal cooling system using air as the medium, cooled and dried air is ventilated inside the microenvironment by a blower. It is the most natural way of cooling, since heat is mainly extracted via natural sweat evaporation and enhanced convection. However, it is limited by dependence on amount of sweat production, low heat capacity of air and poorer control of the cooing rate.

As for a liquid cooling system, cooled liquid flows inside the cooling tubes that are normally woven in or blended with the cooling garment. It is usually worn close to skin and heat is mainly removed by conduction and convection. The cooled liquid can be obtained by ice melting or some refrigeration system. The advantages of liquid cooling

include high heat capacity medium, better control of heat extraction rate, and capability of dealing with high metabolic rates. However, liquid cooling system is limited by potential leakage, condensation and energy required. Table 1.1 shows the advantages and disadvantages of air cooling system, liquid cooling system and ice cooling system**.**

Table 1.1 Advantages and Disadvantages of Air Cooling, Water Cooling and Ice Cooling

Cooling System	**Advantages**	**Disadvantages**
Air	• Employs natural sweat evaporation • Enhances convective cooling • Lightweight • Low power consumption	• Difficult to cool inlet air • Inlet air filtration • Blower design • Depends on sweat output
Liquid	• Sealed system • High heat capacity medium • Control of heat extraction rate • Capable of dealing with high metabolic rates	• Clothing redesign • Weight • Potential leakage • Condensation
Ice	• No Energy required	• Weight • short term cooling

Research Goal

The purpose of this research is to develop a thermal model which can simulate a person thermally interacting with the liquid, air or ice cooling garment and the environment imposed, providing reasonable prediction to the wearer's physiological response, cooling capacity needed, or working time permitted. This research is focused on level A PPE (impermeable). The thermal model will be validated with USF experiment data in various environment conditions, at various work rates and with various clothing ensemble characteristics. Parametric studies will be carried out for water cooling garment and air cooling garment. A typical Extra-vehicular activity (EVA) on Mars will be simulated and the simulation results will be used to design cooling system.

CHAPTER 2 LITERATURE REVIEW

Simple thermal models have been extensively used in the assessment of human in thermal environments. During last century, attempts and efforts were made to combine environmental parameters and physiological variables in developing a unified heat stress index. The existing indexes can be divided into two main categories: effective temperature (ET) scales, which are based on meteorological parameters only (e.g., ambient temperature, wet-bulb temperature, black-globe temperature), and rational heat scales, which include a combination of environmental and physiological parameters (e.g., radiative and convective heat transfer, evaporative capacity of the environment, and metabolic heat production). These methods are relatively simple and the index can be obtained from the use of charts or graphs. However, they lack the capability to adjust for different levels of metabolic rate and different clothing, e.g., protective clothing. The development of digital computers has provided a facility, which allows more detailed models to be used in practical application.

Thermal models provide a mathematical description of human response to thermal environments and it involve both a passive and controlling system for the body as well as mechanisms of heat exchange.

Thermoregulatory Models Review

Around 1970, when substantial data on thermoregulatory control functions became available in the literature, and with the increasing availability of computers, the development of physiological simulation models started. In the past 40 years, more detailed, multi-segmental models of human thermoregulation have been developed. These models combined physics of internal and external heat flow with internal body temperature regulation. The most well known physiological models was created by Stolwijk (1966) and has been a source of motivation for various refinements, improvements and further development. He was followed by many other authors who published relatively simple (Gagge et al., 1977) to more complex (Wissler, 1964, 1982; Werner, 1989; Werner and Webb, 1993) physiological models. Many of these models have been valuable research tools contributing to a deep understanding of the principles of human thermoregulation.

Fanger P.M.V. – P.P.D. Model

The first step was done by Fanger (1970) with the Predicted Mean Vote (PMV) and the Predicted Percentage of Dissatisfied (PPD). PMV is grounded on thermal balance S of the body, between heat produced by metabolism (M-W, where M is total metabolism, W is the external work) and heat exchanged with environment through skin and respiration (E+R+C+Res, where E is sweat evaporation, R and C are the radiative and convective

heat transfer, Res is respiration heat transfer which includes latent and sensible heats). S is related to PMV, a vote scale, which is equal to zero for neutrality (S=0), is positive or negative according to S sign, and varies from –3 (too cold) to +3 (too hot). PPD is deduced from PMV through a chart established after a great number of experiments.

Simulation using a PMV based control is easy to do because the great simplicity of PMV type outputs, but not very helpful because all ambience parameters are reduced to one index and the effects of each of them cannot be analyzed separately. Despite of the great improvements of PMV control versus usual technique, there are still many simplifications for such a method to be sufficient. PMV is used to determine how far from equilibrium the body is, but formulate used to compute it is only valid for equilibrium. A more important drawback of PMV is that it only applies to steady state, in homogenous conditions. A similar result is given when all the body is at neutrality and when simultaneously feet are too hot and head too cold.

A better accuracy in the determination of physiological parameters is given by the use of models, including heat exchanges and physiological thermoregulation processes. The thermal network of the body is made up from a set of nodes, the number of which varying from 2 to about 250. Internal heat exchanges are due to thermal conduction between contiguous layers and to forced convection through blood flow. External heat exchanges include sensible (conduction, convection, radiation) and latent heat (sweat evaporation, respiration). Physiological reactions, in charge of the maintain of a

constant internal temperature, are shivering and vasoconstriction, against cold environment, sweat and vasodilatation against hot climate.

Stolwijk and Hardy 25-node Model

Stolwijk is one of the forerunners in the research of human thermoregulatory model and his model has provided the basis and inspiration for much of the work on thermal modeling. Stolwijk and Hardy 25-node model mathematically represents the geometric and thermal characteristics of the body itself as the passive system, and the temperature information and integration and related physiological controls as the controlling system.

The passive system of the model consists of appropriate sized cylinders representing trunk, arms, hands, legs, and feet; the head is represented as a sphere. Each of these has four concentric layers or compartments representing core, muscle, fat and skin layers. An additional central blood compartment, representing the large arteries and veins, exchanges heat with all other compartments via convective heat transfer occurring when the blood flow to each compartment. The model assumes that the body is symmetric to reduce the number of calculations.

The six segments, four compartments each segment and the central blood compartment make a total 25 nodes. For each of 25 compartments, heat balance

equations was developed to account for heat flow into and out of the compartment, via conduction and convection, and the metabolic heat production within the compartment. The model is based on a standard, 1.72m, 74.4 kg man with a volume of 74.4×10^{-3} m^3.

The controlling system in body temperature regulation consists of three parts. The first part contains the sensing mechanisms which recognize the thermal state of the controlled system. The second part receives information regarding the thermal state, integrates it and sends out appropriate effector commands to the various effector systems. The third part of the controlling system receives the effector commands and modifies them according to the conditions at the periphery before translating such commands into effector action.

In its original form, Stolwijk and Hardy 25-node model represents only the nude body. The model is well validated for hot environments, but it is not applicable to cold exposure.

Nishi and Gagge 2-node Model

A simplified version of Stolwijk and Hardy model was also developed by Nishi and Gagge (1977) in practical application. The human body is considered to be a single cylinder with two concentric layers. The inner layer is the central core and the outer

layer is the skin. The controlling system is represented by a similar system to that used by Stolwijk and Hardy but with only 2 nodes to control. Gagge's model can be used to describe thermoregulatory responses to various environmental and exercise conditions, but accuracy of transient predictions depends almost entirely on time steps used for integration. Gagge's model does not work well if personal cooling is applied to the human body due to the large temperature gradient.

Wissler Model

Wissler (1985) describes a model, which computes 225 temperatures in 15 elements plus O_2, CO_2 and lactate concentrations. The model is an order of magnitude larger than the Stolwijk and Hardy model and it is well validated for hot and cold environments and both atmosphere and hyperbaric environments. The detail provided allows its use in specialist areas such as for cold water immersion and diving, where it has been used in application.

Werner Model

Werner (1989) provides probably the most sophisticated thermal model available. It's three-dimensional and involves 63 types of tissues with the temperature grid in the body (1cm for the trunk, 0.5cm for other parts) represented by 400,000 points. " an unresolved problem is the control strategy of the system, that is the question whether

the inhomogeneous pattern of effector distribution is maintained in the cold and warmth or whether active modification and control is distributed". The model requires a very powerful computer to perform the many calculations involved. It provides detailed results and is supported by a program of research which develops knowledge about both passive and controlling properties.

Clothing Models Review

Clothing provides a thermal resistance between the human body and its environment; so one functional role of clothing is to maintain the body in an acceptable thermal state, in a variety of environments. In some cases, Personal Protective Equipment (PPE) is worn to reduce persons' exposures to hazards when the administrative controls are not feasible or effective in reducing these exposures to acceptable level.

The thermal behavior of clothing in an (active) person is complex and dynamic, not fully understand and difficult to quantify. That does not say that much is not known, there has been much theoretical and empirical research. Factors affecting the thermal behavior of clothing will include the dry thermal insulation, transfer of moisture and vapor through clothing, heat exchange with clothing (conduction, convection, radiation, evaporation and condensation), compression (e.g. caused by high wind), pumping effect (e.g. caused by body movement), air penetration (e.g. through fabrics, vents and openings),

subject posture and so on. An approach to assessing the thermal properties of clothing is to identify simple thermal models of clothing behavior and attempt to estimate values of quantities required for the thermal models.

A Simple Clothing Model

The dry thermal insulation value of clothing materials and clothing ensembles is of fundamental importance and has been extensively investigated. A simple thermal model is of a heated body with a layer of insulation. For the body to maintain equilibrium, heat flows from body to the skin and then through clothing to the environment. The heat flow direction depends on the temperature of body and environment conditions.

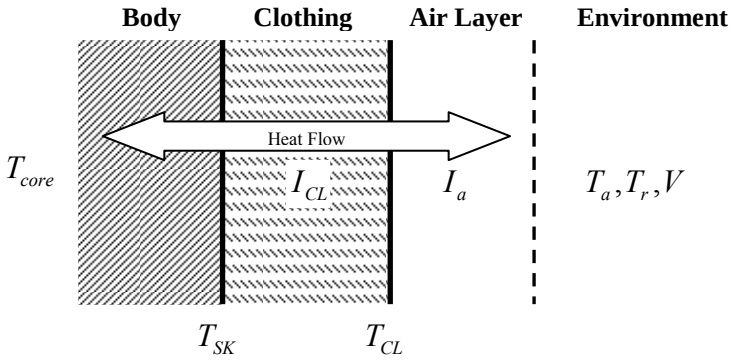

Figure 2.1 A Simple Model with a Layer of Clothing Insulation

The simple model presented (Figure 2.1) provides a representation of clothing in the stationary, comfortable or cold human body in many conditions. It provides only an

approximation however to many circumstance. An important limitation of the model shown here is that it does not consider wet clothing. Moisture can transfer heat between the body and the environment. This is particularly important when the skin sweats.

2-parameter Model

A simple two-parameter model (Figure 2.2) would consider both dry heat transfer and moisture transfer, which combine to provide the total effect.

For most practical applications the simple dry insulation “model” is used to quantify clothing insulation (e.g. Fanger, 1970). For more specialist evaluations of clothing, the two- parameters model is needed especially for the hot environment where sweating and hence vapor permeation properties will be of great importance.

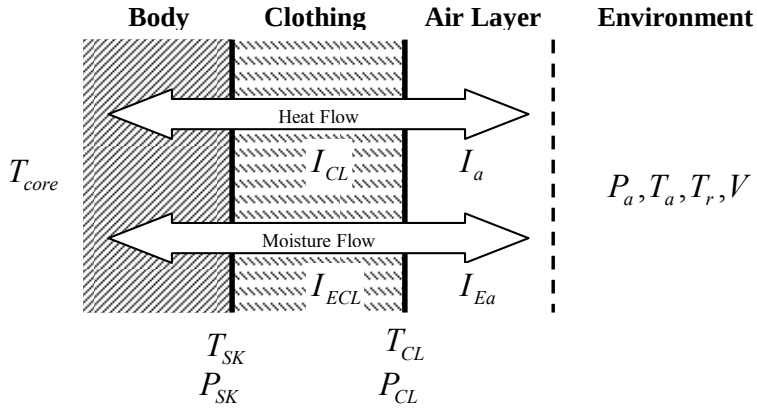

Figure 2.2 2-Parameter Model with a Layer of Clothing Insulation

For a more detailed representation of clothing, models are required which involve other important factors of clothing thermal behavior.

More Complex Model

Factors which are not considered in two- parameters model may have a significant effect on the thermal properties of clothing. Kerslake (1972) noticed that the insulation is provided by the fabrics themselves and the layers of air trapped between the skin and clothing and the clothing layers. The insulation of clothing is mainly decided by the air trapped in and between them.

Other important factors, including wind penetration, pumping, clothing ventilation, wicking, are very difficult to model and depends greatly on the clothing design, thermal conditions of the body and a person's activity. More complex models of clothing can have a number of characteristics in addition to the simple two-parameter model. No fully comprehensive model exists and the possibility for this is restricted.

The thermal properties of fabrics change with the change of temperature, humidity. For a complex transient model, these factors are also required to be considered.

CHAPTER 3 DESCRIPTION OF THERMAL MODEL

It is anticipated that the interpretation of many parameters at a time may be a difficult job. A structured way to show the results of the analysis in a quantitative way is to develop a computer model that includes the observed mechanisms. This will produce the experimentally observed reactions, if correct. For this purpose, an existing model of thermoregulation will be taken as a starting point. Model will be tested by using the data collected from literatures and/or from USF.

Thermoregulatory Model

The model used as a starting point was described by Stolwijk (1977). The thermoregulatory model contains a number of control functions for physiological processes, as well as the heat transfer properties of the human body. Core, muscle, fat and skin temperature are used as input for several set point identified feedback loops controlling effector responses (skin vasoconstriction/dilation, sweat production, shivering). The effector responses together with metabolism due to exercise result in a certain heat loss or gain, which then affects the “passive” system (the body), resulting in a new body temperature (i.e. the feedback). The relation between effectors and

resulting body temperature is affected by environmental parameters (heat transfer properties) and heat production levels (activity). The passive system itself is defined in terms of heat capacity, mass and surface area, which are constants in the original Stolwijk model.

When performing simulations, the original model expects as inputs a time sequence of:

- The climatic parameters: temperature (T), humidity or vapor pressure (P_a), wind speed (v), and additional radiation between environment and skin (rad; e.g. fire or sun).
- The persons activity level, expressed as the external work load and his metabolic rate (excluding the additional effect due to shivering which is generated by the model itself)

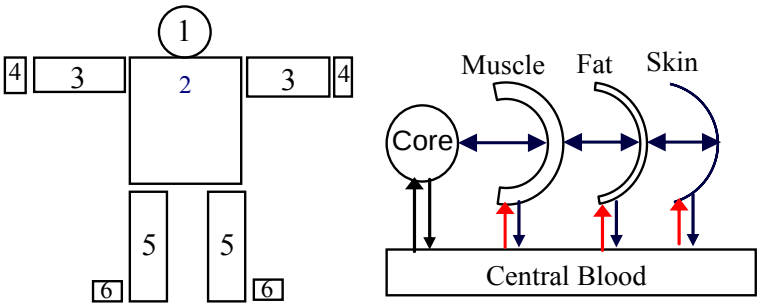

Figure 3.1.Thermoregulatory Model Based on Stolwijk and Hardy

The thermoregulatory model based on Stolwijk and Hardy is schematically shown in Figure 3.1.

The human body is divided into six parts, five appropriately sized cylinders for trunk, arms, hands, legs and feet, and a sphere for head. Each of these parts has four concentric layers or compartments, representing core, muscle, fat and skin layers. An additional central blood compartment exchanges heat via convection to all other compartments. The model assumes that the body is symmetrical to reduce number of the calculations, so there are totally 25 nodes in this model. The output of Stolwijk and Hardy model includes node temperature (total 25 nodes), sweat rate, blood flow rate, etc. Considering the above-mentioned input parameters, it is obvious that the model does not discriminate between different individuals when performing a simulation. It will produce the same output, based on parameter estimations on a group level, whether the subject is small or big, fit or unfit. Thus in order to improve the models performance on this point, changes and additions to the model were made.

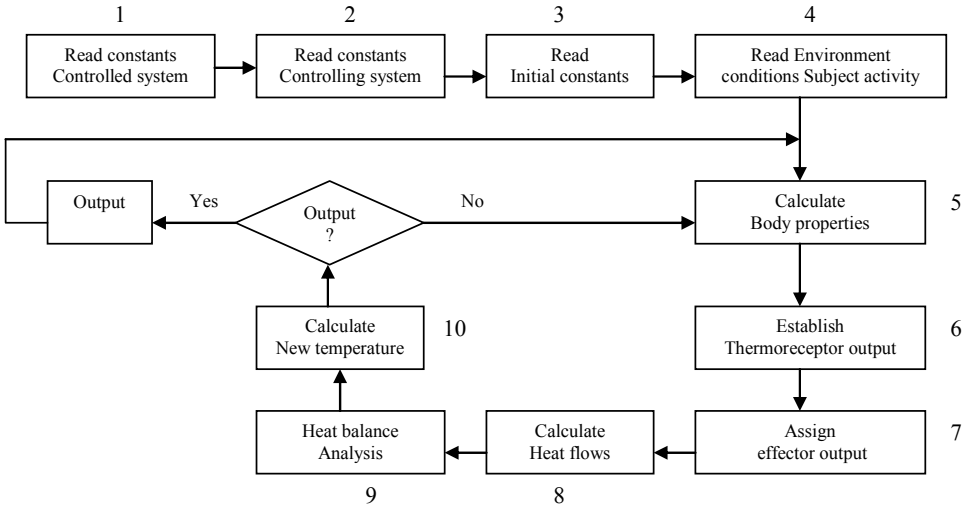

Figure 3.2. Flow Diagram for Various Steps to Implement Model of Thermoregulation in Human Beings

Flow Diagram for various steps to implement model of thermoregulation in human beings is showed in Figure 3.2.

Step 1: Read constants of controlled system. This part reads in the constants which define the controlled system as defined in the tables, such as heat transfer coefficients of each segment, density, conductance, weight, heat capacity of all compartments.

Step 2: Read constants of controlling system. This part reads in the controller constants beginning with the set point temperatures. Set point temperatures are the values of steady state equilibrium temperatures which are obtained under the following conditions: air temperature 29.45 °C, air velocity 0.1 m/s, relative humidity 0.3, basal metabolic rate no regulation.

Step 3: Read initial constants. The initial conditions include the initial values for the temperatures in all compartments. These values are assumed to be same as the set point temperatures which are given in the APPENDIX A, Table A5.

Step 4: Read environment conditions / subject activity. Environment conditions include temperature, relative humidity, and wind speed. Subject activity includes metabolic rate and mechanical efficiency. Metabolic rate is the energy released by the oxidation processes in the human body per unit time. As an estimate of metabolic rate, M, can be

made by measuring how much oxygen has been consumed. This is measured by collecting expired air from human body while performing a task of interest. McIntyre (1980) presents a simple equation based on oxygen used and ventilation rate V.

$$M = 20600V(O_i - O_e) \tag{3.1}$$

where O_e is fraction of oxygen in expired air and O_i is fraction of oxygen in inspired air, normally O_i =0.2093. The metabolic rate has been express as a function of the body surface area A_D. Body surface area, which varies substantially between subjects, directly affects the heat transfer area, and is determined from body mass and height using the equation of DuBois and DuBois (1916):

$$A_D = (Weight^{0.425} - Height^{0.725}) * 0.007184 \tag{3.2}$$

with $Weight$ in kilograms, $Height$ in centimeters and surface area in meter square.

The energy released by oxidation is not all converted to heat, a small part of the energy is used to perform external work, W. The mechanical efficiency of the body doing work is given by:

$$\eta = \frac{W}{M} \tag{3.3}$$

Maximum values of η are around 20-25% and close to zero for many tasks. The metabolic heat production is then calculated by subtracting W from metabolic rate M. The metabolic rate and mechanical efficiency of typical activities can be estimated from the Table B1, APPENDIX B.

Step 5: Calculate body properties. Stolwijk and Hardy model is based on a standard man with a body weight of 74.4 kg and a surface area of 1.89 m^2. The apparent disadvantage of their model is that it will give same simulation result no matter what kind of size the subject is. In order to enable the model to simulate various individual anthropometrics, an input option for the values for mass and height of the subject was added. The effects of these variables on body surface area and body heat capacity were incorporated in the manner explained below.

As body surface area determines heat transfer area and it can vary substantially between subjects, this is an important effect to be incorporated in the model. Body surface area A_D is determined from body mass and height using the equation of DuBois and DuBois (1916). The surface area of each body segment $A(I)$ is expressed as:

$$A(I) = A_{ST}(I) \cdot \frac{A_D}{1.89} \qquad \text{I=1, 2 ...6} \qquad (3.4)$$

Where $A_{ST}(I)$ is the surface area of each body segment for standard man, the values are listed in Table A11, APPENDIX A.

With an increasing A_D, the area for sweat production will also increase. The amount of sweat produced by the body is made dependent of A_D , in a linear fashion, using the standard subject (74.4 kg, 1.89 m^2) as a reference. The same approach has been chosen for skin blood flow and for maximal sweat production and blood flow:

$$SWEAT(I) = SWEAT_{ST}(I) \cdot \frac{A_D}{1.89} \tag{3.5}$$

$$BF(4I) = BF_{ST}(4I) \cdot \frac{A_D}{1.89} \tag{3.6}$$

Body mass mainly determines body heat capacity, relevant for determination of the magnitude of the body temperature change at a certain heat storage rate. The body heat capacity for each compartments are expressed as:

$$C(N) = C_{ST}(N) \cdot \frac{Weight}{74.4} \qquad \text{N=1, 2…25} \tag{3.7}$$

Where $C_{ST}(N)$ is heat capacity of compartment *N* for standard man, the value is listed in Table A1, APPENDIX A.

Step 6: Establish thermoreceptor output. The controlling system consists of a temperature sensing system, an integrating system, and an effector system.

- The temperature sensing system recognizes the thermal state of the controlled system. It is assumed that thermoreceptors are present in all tissues, allowing for maximum flexibility in the evaluation of different thermoregulatory controller concepts.
- The integrating system receives information of the thermal state, integrated it and sends out appropriate effector commands to the various effector systems. Error signals are derived for all compartments as:

$$ERROR(N) = T(N) - TSET(N) + RATE(N) * F(N) \tag{3.8}$$

where *T* represents for temperature, °C; *RATE* for dynamic sensitivity of thermo-receptors; *F* is defined as temperature increase in unit time.

When the value of *ERROR* is positive, warm receptors are effective, and

$$WARM\ (N) = ERROR\ (N) \tag{3.9}$$

When the value of *ERROR* is negative, cold receptors are effective, and

$$COLD\ (N) = -ERROR\ (N) \tag{3.10}$$

WARM and *COLD* are then be integrated into one parameter *WARMS* or *COLDS* with weight factors.

Step 7: Assign effector output. The effector system receives the effector commands and modifies them according to the conditions at the periphery before translating such commands into effector action.

The four controlling signals, namely *SWEAT, DILAT, CHILL* and *STRIC*, indicating behaviors of sweating, vasodilation, vasoconstriction and shivering respectively, are given as:

$$SWEAT = CSW * ERROR(1) + SSW * (WARMS - COLDS) + PSW * WARM(1) * WARMS \tag{3.11}$$

$$DILAT = CDIL * ERROR(1) + SDIL * (WARMS - COLDS) + PDIL * WARM(1) * WARMS \tag{3.12}$$

$$CHILL = (CCHIL * ERROR(1) + SCHIL * (COLDS - WARMS)) * PCHIL * (WARMS - COLDS)$$

(3.13)

$$STRIC = CCON * ERROR(1) + SCON * (COLDS - WARMS) + PCON * COLD(1) * COLDS$$

(3.14)

where *CSW,SSW, CDIL, SDIL, CCON, SCON, CCHIL, SCHIL, PSW, PDIL, PCON* are control coefficients.

During vasodilatation, venous blood returns near to the skin hence increasing the availability of heat loss from the skin to the environment. Vasoconstriction enables constriction of superficial veins so that cool blood from the skin returns along the venae comitans close to the artery, hence gaining heat and returning to the body core. Shivering can increase metabolic heat production and make core temperature dropping slower. Sweating is the process that, when the body temperature rises, sweat is secreted over the skin to allow cooling by evaporation. (Parsons, 1993)

The resting metabolic rate is assumed 86.5 W for the whole standard man. The basal metabolic assigned to all the core layers are assumed not to vary under the relatively short-term conditions for which the model will be used, as well as for the fat layers and skin layers.

$$M_{core} = M_{core\_basal} \quad \text{(for all the 6 core nodes)} \quad (3.15)$$

$$M_{fat} = M_{fat\_basal} \quad \text{(for all the 6 fat nodes)} \quad (3.16)$$

$$M_{skin} = M_{skin\_basal} \quad \text{(for all the 6 skin nodes)} \quad (3.17)$$

The metabolic heat production in the muscle layers is the sum of the basal rate of heat production, and the heat production due to muscular work and any shivering thermogenesis.

$$M_{muscle} = M_{muscle\_basal} + WORKM(I) * WORK + CHILM(I) * CHILL \quad (3.18)$$

where $$WORK = (M - 86.5) * (1 - \eta) \quad (3.19)$$

η is the efficiency of mechanical work; *WORKM* and *CHILM* are weighting factors.

Due to limitation on measurement data, certain simplifications are made for the redistribution of blood flow. It is assumed that blood flow to the core and fat layers remains at the basal values:

$$BF(N) = BFB(N) \quad (3.20)$$

$$BF(N+2) = BFB(N+2) \quad (3.21)$$

The muscle compartments have wide variation in blood flow, which is approximately represented as:

$$BF(N+1) = BFB(N+1) + M_{muscle} - M_{muscle\_basal} \quad (3.22)$$

the skin blood flow is highly dependent on the termoregulatory controller, expressed as:

$$BF(N+3) = \frac{BFB(N+3) + SKINV(I) * DILAT}{1 + SKINC(I) * STRIC} * 2^{\left(\frac{ERROR(N+3)}{10}\right)} \quad (3.23)$$

where *SKINV* and *SKINC* are weighting factors.

Step 8: Calculate heat flows. This part computes the net heat flow rates into or out of each compartment. The convective heat transfer by blood flow plays a most important role in the thermal responses to internal and external stresses:

$$Q_{blood} = BF(N) * (T(N) - T(25)) * \rho * C \quad (3.24)$$

where ρ and C represent for density and specific heat of blood. The value are shown Table A1 and A2, APPENDIX A.

Thermal conductance between layers in each segment can be calculated with the aid of data provided by Stolwijk and Hardy.

$$Q_{cond.} = k\Delta T_{neighbor} \quad \text{(for all the 24 nodes)} \quad (3.25)$$

where k is the thermal conductity for each of the 24 node, with values shown in Table A3, APPENDIX A. $\Delta T_{neighbor}$ represents the temperature difference between the correspondent two neighboring nodes.

Inspired air is both warmed and humidified on its passage to the lungs, where it reachs almost complete satuation at a temperature equal to trunk core temperature. When the air moves outward through the respiratory tract some heat is transferred back to the body and water is partly condensed, but the expired air still contains more heat and water than the inspired air. Breathing therefore results in a latent heat loss and a sensible heat loss from the trunk core. Fanger (1970) provided useful equations to calculate both sensible heat loss and latent heat loss.

For sensible heat loss (W):

$$C_{res} = 0.0014M(34 - T_{in}) \tag{3.26}$$

For latent heat loss (W):

$$E_{res} = 0.0017M(58.6 - p_{in}) \tag{3.27}$$

Where p_{in} is partial pressure of water vapor in inspired air (mb)

T_{in} is inspired air temperature (°C)

In the evaporative heat loss process, the water is brought to skin surface by sweat glands where it evaporates and passes through the clothing to the environment. If the ambient humidity is low and the vapor resistance of the clothing is small, the evaporation takes place at the top of gland and the skin remains relatively dry. Otherwise the skin continues accumulating sweat and the skin may be totally wetted. If the skin is completely covered by water, the vapor pressure next to the skin equals the satuation pressure of water at skin temperature. The maximum evapation rate happens when the vapor pressure reachs satuation.

$$E_{\max} = (P_{skin} - P_{mem}) \cdot h_e \tag{3.28}$$

Where $h_e = 2.2h_c$

Stolwijk and Hardy provided experienced equation to calculate actual evaporative heat loss from the skin.

$$E_{skin} = E_{skin\_basal} + SkinS * SWEAT * 2^{\frac{T_{skin} - T_{skin\_set}}{BULL}} \tag{3.29}$$

Where *SkinS* represents 6 weighting factors and *BULL* is the control coefficient. It is obvious that actual evaporative heat loss could not be larger than the maximum

evaporation rate at any time. If any evaporative heat in E_{skin} exceeds its coresponding max value, then it must be reduced to $E_{\max}$. There is no evaporative heat loss occurred in fat, muscle and core layer except trunk core.

Step 9: Heat balance analysis. Heat balance is obtained for each node of all the 6 core nodes at every time level:

$$Q_{core} = M_{core} - E_{res} - C_{res.} - Q_{blood} - Q_{cond.} \quad (3.30)$$

It should be noted that the respiratory heat loss $E_{resp.}$ and $Q_{resp.}$ only occure in the trunk.

$$Q_{muscle} = M_{muscle} - Q_{blood} - Q_{cond.} \quad \text{(for all the 6 muscle nodes)} \quad (3.31)$$

$$Q_{fat} = M_{fat} - Q_{fat} - Q_{cond.} \quad \text{(for all the 6 fat nodes)} \quad (3.32)$$

$$Q_{skin} = M_{skin} - E_{skin.} - Q_{blood} - Q_{cond.} - Q_{cond\_en.} - Q_{conv\_en.} - Q_{rad\_en.} \quad (3.33)$$

(for all the 6 core nodes)

The total heat from blood can be expressed as:

$$Q_{blood\_total} = \sum_{1}^{24} Q_{blood} - 0.08 * Work \quad (3.34)$$

Step 10: Calculate new temperatures. After the analysis of heat balance, temperatures differences for the 25 nodes can be calculated and then temperatures are updated as:

$$T_{new} = \frac{Q}{C} * \Delta time + T \ (°C) \quad (3.35)$$

Description of Cooling Garment Model

As mentioned in chapter 2, many factors have to be considered in complex clothing model. The interaction between penetration, pumping, clothing ventilation and thermal insulation of fabrics are very difficult to model and depends greatly on clothing design. Since the dissertation mainly deals with impermeable coverall clothing, where wind penetration, pumping and clothing ventilation are not possible to happen, and these effects are not considered in the thermal model.

Water Cooling Garment Model

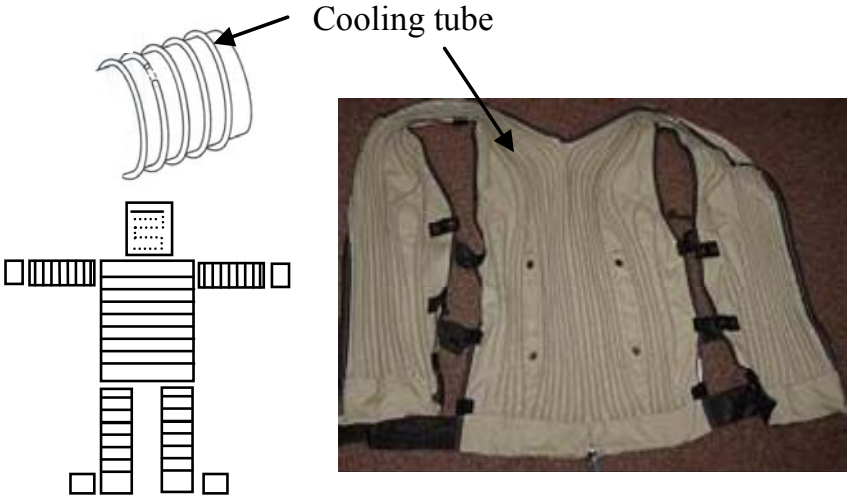

Figure 3.3. Schematic Arrangement of the Tubing for Water Cooling Garment

Liquid-cooled garment was first developed to protect the Apollo astronauts from the high temperatures on the moon. The garment successfully maintained the astronauts' body

temperatures at a comfortable level by utilizing a battery-powered mini-pump to circulate chilled water through a network of tubes in the garment.

Water cooling garment was worn close to skin. Figure 3.3 shows the schematic arrangement of the water cooling garment tubing and picture of commercial available water cooling garment. The thermal resistance network is showed in Figure 3.4, the resistance calculations are listed below.

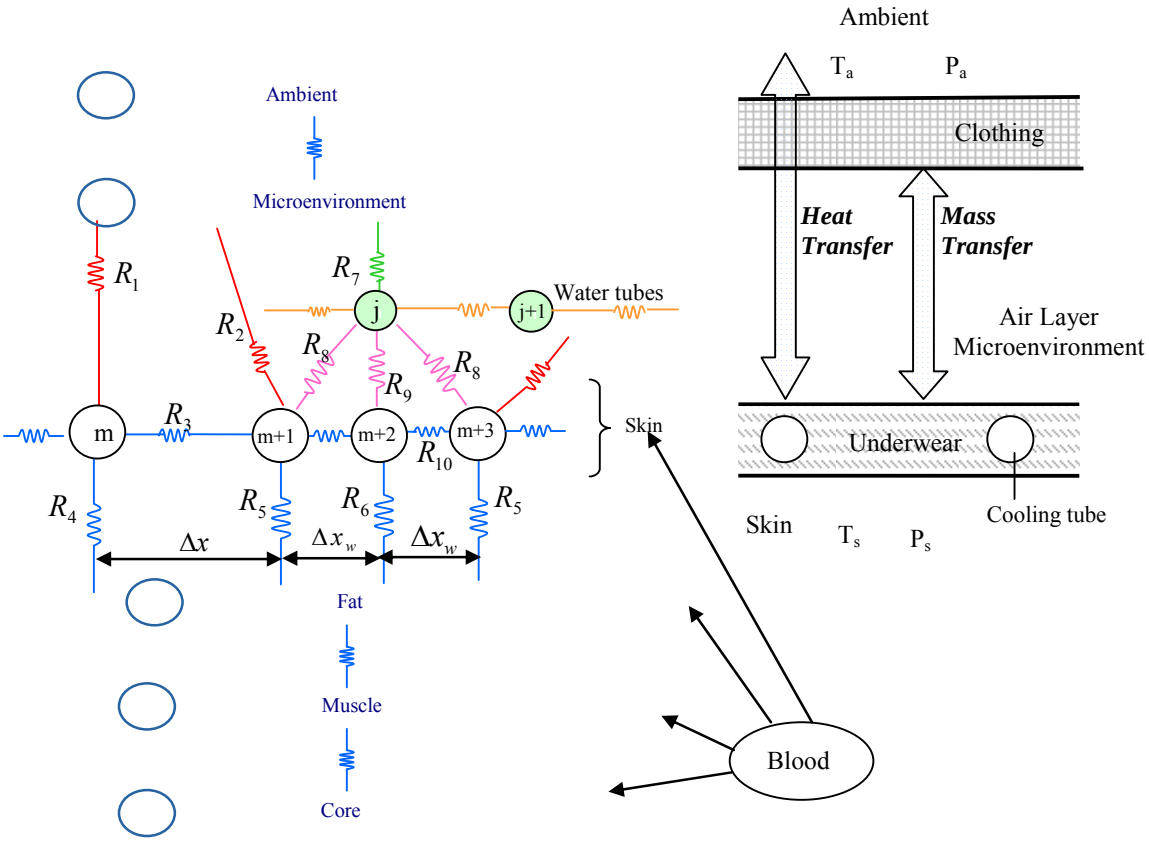

Figure 3.4 Thermal Resistance Network of Thermal Model

Thermal Resistance Between Skin Nodes (R3 And R10)

The thermal resistance depends on the distance between two neighboring nodes and skin thermal conductance,

$$R_3 = \frac{\Delta x}{k_{skin} A_3} \tag{3.36}$$

$$R_{10} = \frac{\Delta x_w}{k_{skin} A_{10}} \tag{3.37}$$

Where k_{skin} is skin thermal conductivity which is listed in Table A3, APPENDIX A; Δx and Δx_w are distanced between two neighboring nodes as shown in Figure 3.4, Δx_w equals to half of tube diameter; A_3 and A_{10} are corresponding heat transfer areas which are define as:

$$A_3 = \pi(r_{skin}^2 - r_{fat}^2) \tag{3.38}$$

And

$$A_{10} = \pi(r_{skin}^2 - r_{fat}^2) \tag{3.39}$$

r_{skin} represents the radius of body part; r_{fat} represents the radius of fat layer, the values of r_{skin} and r_{fat} for standard man can be obtained from Table A10, APPENDIX A.

Thermal Resistance Between Skin And Fat (R4, R5 And R6)

The Stolwijk and Hardy thermoregulatory model provides the thermal conductance between the compartments, as long as we know the heat transfer area between the adjacent nodes, we could obtain the value of R_4, R_5 and R_6.

$$R_4 = \frac{S}{A_4 k_{skin-fat}} \tag{3.40}$$

$$R_5 = \frac{S}{A_5 k_{skin-fat}} \tag{3.41}$$

$$R_6 = \frac{S}{A_6 k_{skin-fat}} \tag{3.42}$$

Where S is the total heat transfer area between skin and fat for each segment. $k_{skin-fat}$ is the thermal conductance between fat and skin, the value of thermal conductance is listed in Table A14, APPENDIX A. A_4, A_5 and A_6 are defined as:

$$A_4 = 2\pi \frac{r_{skin} + r_{fat}}{2} \Delta x \tag{3.43}$$

$$A_5 = 2\pi \frac{r_{skin} + r_{fat}}{2} (\frac{\Delta x + \Delta x_w}{2}) \tag{3.44}$$

$$A_6 = 2\pi \frac{r_{skin} + r_{fat}}{2} \Delta x_w \tag{3.45}$$

Thermal Resistance Between Skin And Microenvironment (R1 And R2)

$$R_1 = \frac{1}{hA_1} + R_{cloth} \tag{3.46}$$

$$R_2 = \frac{1}{hA_2} + R_{cloth} \tag{3.47}$$

Where R_{cloth} is thermal resistance of cooling garment; $A_1 = 2\pi r_{skin} \Delta x$, $A_2 = 2\pi r_{skin} \frac{\Delta x}{2}$; h is the combined heat transfer coefficient from the skin to the air of microenvironment. It is noted that, in this model, conduction and radiation are ignored inside the PPE and $h = h_c$.

Thermal Resistance Between Water And Microenvironment (R7)

$$R_7 = \frac{1}{h_w A_{w7}} + \frac{1}{hA_7} + R_{cloth7} + R_{tube\_wall7} \tag{3.48}$$

where

$$A_7 = 2\pi r_{skin}(\pi \frac{D_{tube\_outside}}{2}) \tag{3.49}$$

and the area of convective heat transfer for the water side,

$$A_w = 2\pi r_{skin}(\pi \frac{D_{tube\_inside}}{2}) \tag{3.50}$$

R_{tube_wall} is the thermal resistance of the tube wall,

$$R_{tube\_wall7} = \frac{thickness_{tube}}{k_{tube}(\frac{A_7 + A_{w7}}{2})} \tag{3.51}$$

and

$$R_{cloth7} = \frac{thickness_{cloth}}{k_{cloth} A_7} \tag{3.52}$$

k_{tube}, k_w are thermal conductivities of the tube and water respectively, W/(m°C). The convective heat transfer coefficient for the water can be obtained from

$$h_w = \frac{Nu \cdot k_w}{D_{tube}}, \text{ W/(m°C)} \tag{3.53}$$

The Nusselt Number is then obtained by the following empirical relation:

$$Nu = 0.023\,\mathrm{Re}^{0.8}\,\mathrm{Pr}^{0.4} \tag{3.54}$$

Although the above relation is normally only for $\mathrm{Re} = 10^4 \sim 1.2 \times 10^5$, it is employed in this

study for all the cases. The values of Re observed in simulation are ranged from 2500~20000.

Thermal Resistance Between Skin And Water (R8, R9)

$$R_8 = \frac{1}{h_w A_{w8}} + R_{cloth8} + R_{tube\_wall8} \tag{3.55}$$

$$R_9 = \frac{1}{h_w A_{w9}} + R_{cloth9} + R_{tube\_wall9} \tag{3.56}$$

where $A_{w8} = 2\pi r_{skin}(\frac{\Delta x_w}{2})$, $A_8 = 2\pi r_{skin}(\pi \frac{D_{tube\_outside}}{8})$, $R_{cloth8} = \frac{thickness_{cloth}}{k_{cloth} A_8}$, and

$R_{tube\_wall8} = \frac{thickness_{tube}}{k_{tube}(\frac{A_8 + A_{w8}}{2})}$; $A_{w9} = 2\pi r_{skin}\Delta x_w$, $A_9 = 2\pi r_{skin}(\pi \frac{D_{tube\_outside}}{4})$, $R_{cloth9} = \frac{thickness_{cloth}}{k_{cloth} A_9}$,

and $R_{tube\_wall9} = \frac{thickness_{tube}}{k_{tube}(\frac{A_9 + A_{w9}}{2})}$.

Thermal Resistance Between Microenvironment And Ambient

The thermal resistance between microenvironment and ambient is highly dependent on the thermal resistance of personal protective garment and the heat transfer between PPE and ambient.

The thermal resistance of PPE is estimated by Table C1, APPENDIX C. Heat transfer between PPE and ambient will be talked later.

Air Cooling Garment Model

The air cooling garment is supplied with a flow of cool air which is distributed over the body by a system of ducts or by spacer garment. For permeable suits, air may exit the clothing through fabric and at openings such as neck, wrist and ankles. Impermeable clothing generally have one-way valves to dump air to environment. shows the air distribution vest and personal cooling conditioner made by Encon. The cooling conditioner is capable of producing about a 40°F drop from incoming air temperature.

Air cooling can be applied to the whole body or only certain body parts according to the requirement of the application. With the air cooling system employed inside the PPE, the heat will be removed from the human body and warmer ambient through two methods, one is sensible heat transfer (convection) and the other is latent heat transfer (evaporation). Factors which determine air cooling garment performance include the temperature and humidity of the air supply, mass flow rate and the effective surface area available for heat exchange. Due to the specific heat of air, convective cooling is a relatively weak mechanism. Theoretically, cooling could be improved by supplying extremely cold air, but in practice, too cold inlet air may result in local skin discomfort. Evaporation is a strong cooling mechanism because of high sweat vaporization heat, which makes the latent heat transfer a dominating term in the whole heat removal. Air flow through the suit is limited by problems of noise, wind and a tendency for the suit to develop positive pressure and inflate to awkward bulkiness.

Figure 3.5 Air Distribution Vest and Personal Cooling Conditioner by Encon

The control volume method is used for the numerical calculation. Because the air will pick up a lot of moisture and heat from human body, which makes air relative humidity change a lot. So the flowing air is uniformly divided into small segments along its flow passage. The body skin was also divided into small segments to calculate the skin temperature distribution.

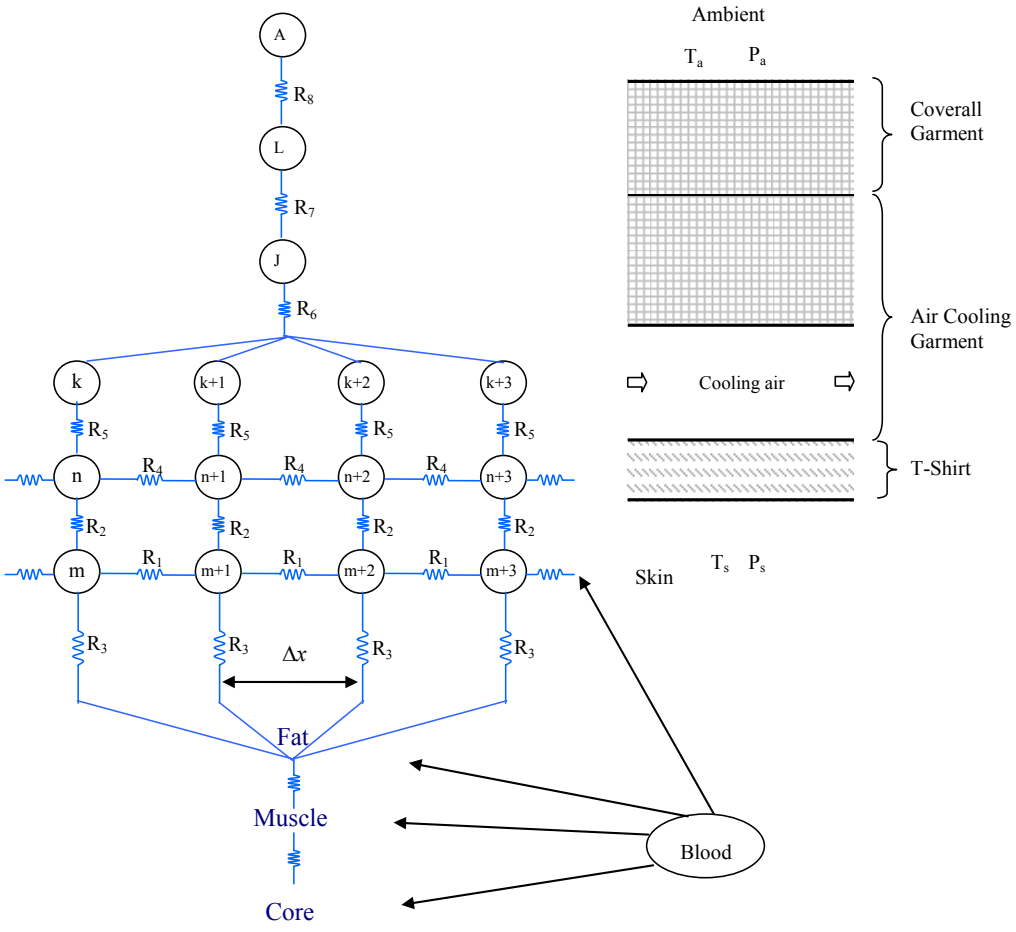

Figure 3.6. Air Cooling Garment Nodes Network

Figure 3.6 shows the node network of air cooling model, the resistance calculation is similar to the water cooling model.

Since the nodes are divided evenly for the air and skin layers, the calculation of heat resistance depends on the number of nodes divided in both layers. The heat

conductivity between fat and muscle is provided in Stolwijk thermoregulatory model along with the heat conductivity between muscle and core.

Thermal Resistance Between Skin Nodes (R1)

$$R_1 = \frac{\Delta x}{k_{skin} A_1} \tag{3.57}$$

where A_1 is the heat transfer area involved, and k_{skin} is the thermal conductivity of skin, W/(m °C).

Thermal Resistance Between Skin And T-Shirt (R2)

$$R_2 = \frac{num}{2} \times R_{t-shirt} \tag{3.58}$$

where $R_{t-shirt}$ is the heat resistance of the T-shirt and *num* is the number of nodes for skin layer. $R_{t-shirt}$ can be estimated from Table C1, APPENDIX C.

Thermal Resistance Between Skin And Fat (R3)

$$R_3 = num * R_{skin\_fat} \tag{3.59}$$

where *num* is the number of nodes on skin layer and R_{skin_fat} is the heat resistance between skin and fat, W/(m°C), which is provided in Stolwijk thermoregulatory model.

Thermal Resistance Between T-Shirt Nodes (R4)

R_4 is calculated similarly with R_1.

$$R_4 = \frac{\Delta x}{k_{TS} A_4} \tag{3.60}$$

Where A_4 is the heat transfer area involved, and k_{TS} is the thermal conductivity of T-shirt, W/(m °C).

Thermal Resistance Between T-Shirt And Cooling Air(R5)

$$R_5 = \frac{1}{hA_5} + \frac{R_{t-shirt}}{2} \tag{3.61}$$

where h is convective heat transfer between the T-shirt and the cooling air, which can be obtained from $h_{air} = \frac{Nu \cdot k_{air}}{D}$.

Thermal Resistance Between Cooling Garment And Cooling Air (R6)

$$R_6 = \frac{1}{hA_6} + \frac{R_{CG}}{2} \tag{3.62}$$

where h is convective heat transfer between the T-shirt and the cooling air, R_{CG} is heat resistance of cooling garment, it can be estimated from Table C1, APPENDIX C.

Thermal Resistance Between Cooling Garment And Coverall Clothing (R7)

$$R_7 = \left(R_{CG} + R_{\text{cov}erall} \right) / 2 \tag{3.63}$$

Ice Cooling Vest Model

The ice vest was an ice –cooling garment that was donned over the head and closed around the torso by two straps on each side. The vest construction was heavy cotton with a layer of Thinsulate® insulation against outside heat. There were three horizontal pockets on the front and on the back that contained the ice in a water-gel form. The ice vest weighed about 0.7 kg (1.5 lb) empty and 5.2 kg (11.5 lb) fully charged with9-oz packets 3 attached packets to a pack or one row). Cooling was accomplished by conduction from the skin to the ice packs. Figure 3.7 shows the personal ice cooling vest and blue ice.

Figure 3.7. Personal Ice Cooling Vest and Blue Ice

During the experiments, the ice vest was worn over a cotton tee shirt; according to manufacturer's instructions, thermo sensors were placed in the middle of three different rows between the ice packs and the inner surface of the pocket. When the temperature of two of the three thermo sensors reached 10 °C (50 °F), the ice packs were checked manually. If most of the packs were melted, the ice vest was recharged. The protective coveralls were cut open to gain access to the pocket openings, the ice packs were replaced, and the garment was taped closed. This was accomplished while the subjects continued to walk.

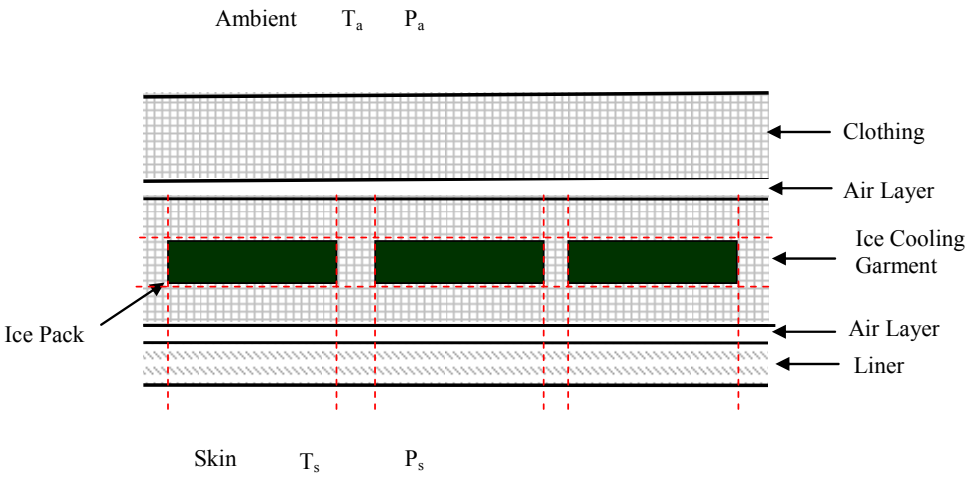

Figure 3.8. Ice Personal Cooling Vest

Ice cooling model includes several layers (liner layer, ice cooling garments layer and clothing layer), the clothing layer is considered as one node in the model due to its high heat transfer resistance and low vapor permeability. The ice cooling garment layer is further divided into 3 sublayers and each sublayer is divided into seven nodes in the model. The air layer in the above figure is not considered as independent layer, but the heat resistance and vapor transfer resistance caused by the air layer are not ignored. Figure 3.9 shows the nodes network of ice cooling model; the resistance calculation is similar with water cooling model.

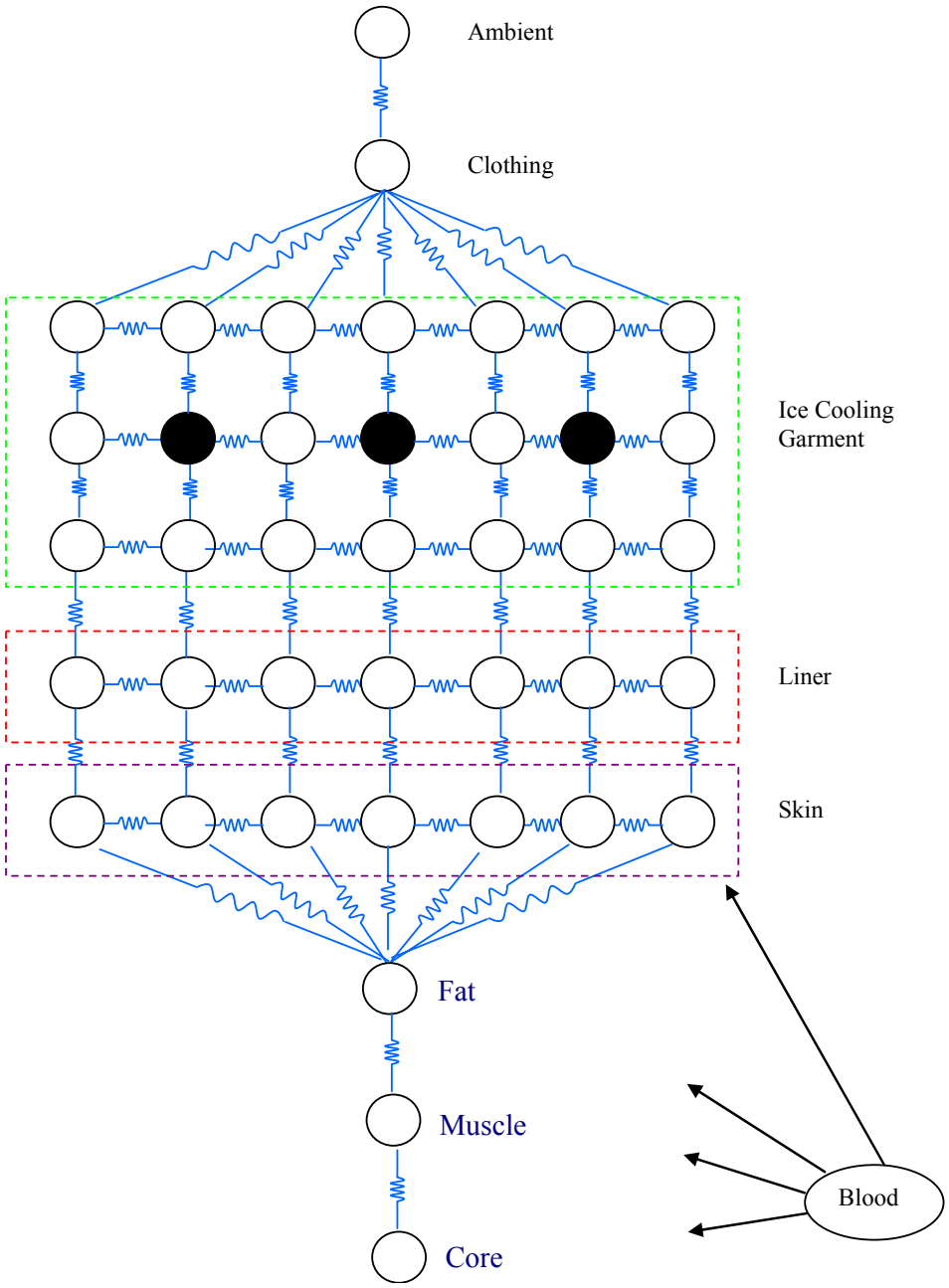

Figure 3.9. Ice Cooling Model Nodes Network

Heat Balance Calculation

For cooling water/air nodes, a steady state is assumed for every time level,

$$T_{j+1}^{i} = T_{j}^{i} + (\sum q_{to\_j}) / (m\ c) \tag{3.64}$$

where j represents the j^{th} cooling water/air node, m is the mass flow rate of cooling water/air (kg/s), c is the specific heat of cooling water/air (J kg^{-1} K^{-1}), and $\sum q_{to\_j}$ is the summary of heat entering the j^{th} cooling water/air node. For cooling node, relative humidity of downstream air is calculated based on that of upstream.

$$RH_{j+1} = f(RH_{j}, m, ms) \tag{3.65}$$

Where RH_j is the relative humidity of cooling upstream air. ms is the mass of sweat removed from skin at node J.

For ice nodes, the temperature is calculated by the following equations.

$$m_{ice}^{i+1} = m_{ice}^{i} - \frac{\sum q_{to\_j}}{H_f} \qquad \text{if ice is not totally melted} \tag{3.66}$$

$$T_{j}^{i+1} = T_{j}^{i} + (\sum q_{to\_j}) / (m\ c) \qquad \text{if ice is totally melted} \tag{3.67}$$

Where m_{ice}^{i+1} is the mass of ice which is not melted at time step (i+1); $\sum q_{to\_j}$ is the summary of heat entering the ice node; and H_f is fusion heat of ice.

For skin nodes,

$$\sum_n \frac{T_n^i - T_m^i}{R_{nm}} + \dot{Q}_{metabolic} + \dot{Q}_{blood} + \dot{Q}_{evap.} = \rho_m c_m \Delta V_m \frac{T_m^{i+1} - T_m^i}{\Delta t} \tag{3.68}$$

where T represents for temperature, ρ for density (kg/m^3), c represents the specific heat capacity of skin (J kg^{-1} K^{-1}), and ΔV represents for volume of the skin node(m^3). Superscript i is for i_th time level, Δt for time step, and subscript m is the node being studied and n for neighboring nodes of m. The first summarized term is based on the assumption that the skin nodes receive conducted heat from the fat layer and neighboring skin nodes. Total metabolic production and blood flow rate in the skin layer are divided according to the volume of each skin node. $\dot{Q}_{metabolic}$ is the metabolic heat production in the controlled volume. $\dot{Q}_{blood}$ is the heat transported by blood to the controlled volume. $\dot{Q}_{evap.}$ is latent heat removal from the skin surface of the control volume by cooling air/water/ice.

Heat Transfer from Clothing to Environment

For a clothed person, there are several parallel pathways for heat loss from core of body:

- evaporation from the respiratory system to environment;
- convection from the respiratory system to environment;
- heat transfer through tissues to the skin surface.

At the skin surface, heat may be removed by conduction, convection and radiation, whereas sweat is removed by diffusion through clothes and by convection at the clothing surface. For clothed person, the heat is removed on clothing surface by convection and radiation.

Convection

Convective heat loss at the surface of the human body has been studied for many years. Convection is usually calculated by means of simplified equation

$$Q_{conv} = A_{suit} h_c (T_{cl} - T_a) \tag{3.69}$$

Where $A_{suit} = f_c A_{nude}$, T_{cl} is clothing outside temperature; T_a is environment temperature. The surface area of nude body is calculated by equation 3.2.

The clothing surface area correction factor has been found experimentally to be

$$f_c = 1.00 + \frac{1.27}{\lambda} \tag{3.70}$$

Where λ is overall conductance of clothing (W/m^{2}K)

Fanger (1970) suggested the following relations for convective heat transfer coefficient h_c:

for the case of free convection

$$h_c = 2.05(T_{cl} - T_a)^{0.25} \quad \text{, kcal/(hr m}^2\ ^\circ\text{C)} \tag{3.71}$$

for the case of force convection (relative air velocity $v < 2.6m/s$)

$$h_c = 10.4\sqrt{v} \tag{3.72}$$

All above equations do not account for pumping effect due to wearer motion. Goldman and co-workers addressed this problem in several studies and provided a series of correction equations to wind and body motion by introducing effective air velocity. The effective air velocity was the combined net effect of wind and increased air motion due to activity (metabolic rate). Based on experimental studies, the following expression was derived (Breckenridge, 1977).

$$v_{eff} = v + 0.004 \times (M - 105) \tag{3.73}$$

with v in m/s and M in Watts.

Radiation

Radiant heat exchange takes place between the human body and its surroundings, just as between two physical objects. The heat loss by radiation from the outer surface of clothed body can therefore be expressed by Stefan-Boltzmann's law:

$$Q_{rad} = A_{eff}\varepsilon\sigma\left(T_{cl}^4 - T_m^4\right) \tag{3.74}$$

Where

ε is the emittance of the outer surface of the clothed body

σ is the Stefan-Boltzmann constant

T_m is mean radiant temperature (°C)

A_{eff} is the effective radiation area of the clothed body (m^2)

$$A_{eff} = f_{eff} \cdot A_{suit} \tag{3.75}$$

f_{eff} is the effective radiation area factor. Fanger (1970) found the effective radiation area factor was around 0.696 for sedentary body posture and 0.725 for standing posture, and these values are independent of sex, weight, height or DuBois area.

Combination of Models

The thermoregulatory model, liquid/Air/Ice cooling garment model and heat/mass transfer calculation involved have been combined together into an integrated model, which can simulate human responses to liquid cooling with impermeable PPE. Figure 3.11 shows the flow chart of the whole thermal model.

Numerical calculation begins with initial conditions prescribed, including the human body initial thermal condition, physical parameters, ambient conditions, and parameters of cooling system. For each time step, core temperatures, weighted body temperature, sweat rate, skin temperatures, microenvironment temperature and humidity for impermeable PPE, are monitored and checked with set acceptable criteria to make sure that heat stress would not occur.

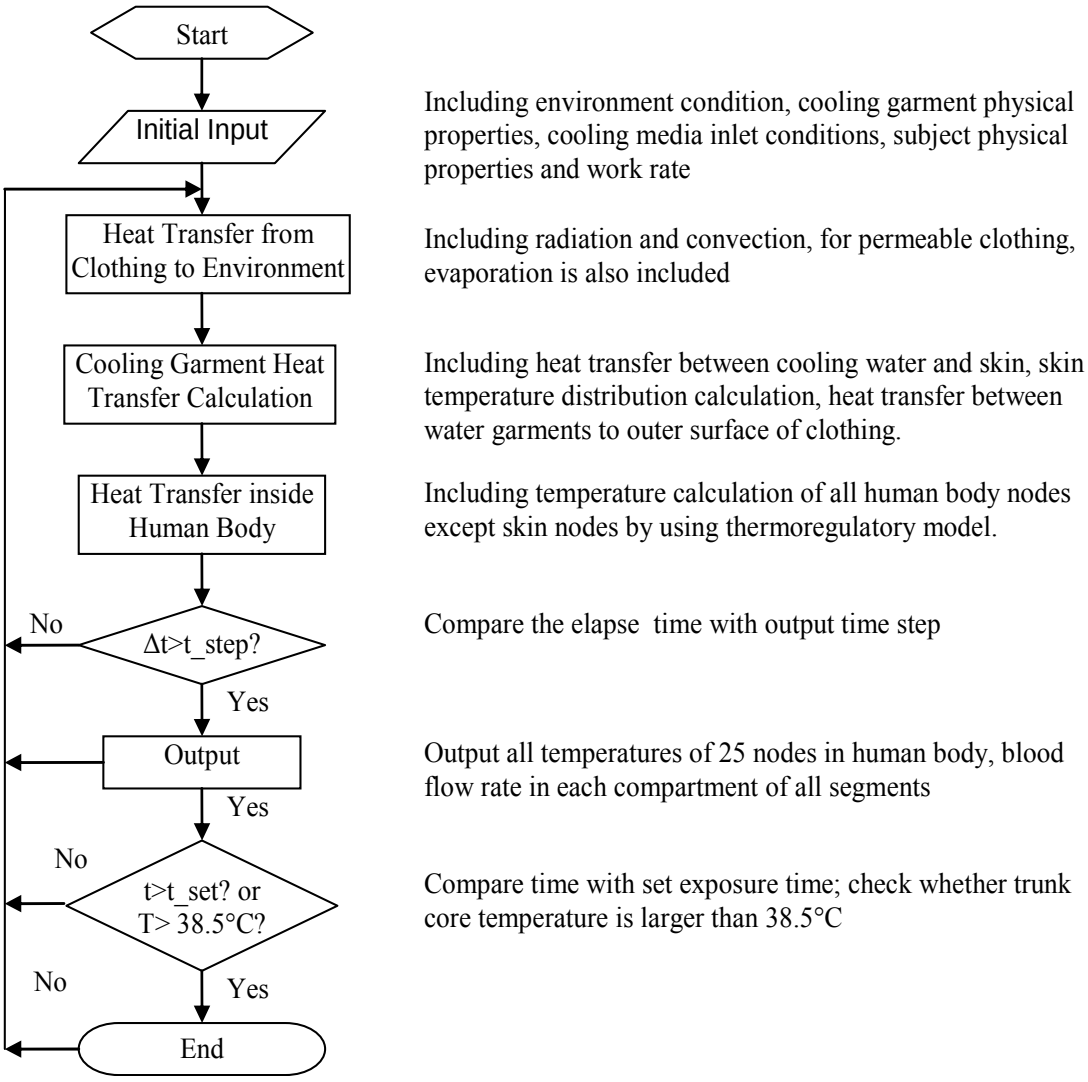

Figure 3.10 Flow Chart of Whole Thermal Model

Water Cooling Lumped Model

Lumped model, which considers the human body as one node with uniform temperature, provides an easy and convenient prediction for human body. Maximum exposure time is

the time for trunk core temperature to reach 38.5 ºC. The lumped model calculation is showed in the following equation.

$$mc\frac{dT_b}{dt} = M(1-\eta) - \frac{(T_b - T_{w,in})}{\sum R_i} - \frac{(T_b - T_{env})}{\sum R_j} \tag{3.76}$$

Where m is human body mass, c is average specific heat capacity of human body, M is metabolic rate, η is mechanical efficiency, T_b is average body temperature, $T_{w,in}$ s is cooling water inlet temperature, T_{env} is environment temperature, where $\sum R_i$ and $\sum R_j$ are heat resistances. The overall thermal resistance between human body and cooling water for lumped model was calculated by adding all the thermal resistances of the thermal model in parallel.

$$\frac{1}{\sum R_i} = \sum_1^p n_p \left(\frac{2}{R_8} + \frac{1}{R_9} \right) \tag{3.77}$$

$$\frac{1}{\sum R_j} = \sum_1^p n_p \left(\frac{2}{R_2} + \frac{1}{R_1} \right) \tag{3.78}$$

Where p is the number of body parts which is covered by cooling tubes; n_p is the number of cooling tube circles on that body part. R_1, R_2, R_8 and R_9 are shown in Figure 3.4.

CHAPTER 4 THERMAL MODEL VALIDATION

The simulations are carried out based on the USF experiment conditions. The results, including core temperatures, skin temperatures, heat removed by cooling system, are selected to be compared with simulation results. The discrepancy between simulation results and experiment data is discussed.

USF Experiment Descriptions

USF Experimental Conditions

The experiment (Fernandes, 2002) was carried out in a climatic chamber. The inside dimensions of the chamber were 2.7 *m* wide, 3.0 *m* deep and 2.2 *m* high. Air speed was 0.5 *m/s*. the dry bulb temperature and wet bulb temperature were held constant to within 0.2 °C. T_{db} = 38 °C, T_{wb} = 30 °C and relative humidity is 60%. There is no radiant heat load and WBGT= 32 °C.

Metabolic rate was controlled by walking on a treadmill by setting a different speed without grade. The subjects were constant walking, with no interruptions.

The standard clothing and personal protective equipment were a polyethylene-coated Tyvek coverall with hood over gym shorts, tee shirt, gym shoes, socks, rubber gloves, and an MSA Ultra Twin respirator with GMC-H cartridge. Hand and ankle cuffs were taped closed and the hood was taped to the facemask.

Personal Cooling Systems Used in USF Experiment

Nine personal cooling systems were evaluated in the experiment; five of them will be discussed in this dissertation.

- Core-Control Suit (CCS): Liquid cooling system that covers the head, trunk, arms and legs. The cooling liquid (water) was circulated through approximately 76 *m* of PVC tubing with about 2 *cm* spacing. The weight of the garment is 1.1 kg.
- Core-Control Jacket (CCJ): Liquid cooling system that covers trunk and arms. The cooling liquid (water) was circulated through approximately 43 *m* of PVC tubing with about 2 *cm* spacing. The weight of the garment is 0.85 kg.
- Core-Control Vest (CCV): Liquid cooling system that covers trunk. The cooling liquid (water) was circulated through approximately 31 *m* of PVC tubing with about 2 *cm* spacing. The weight of the garment is 0.6 kg.
- Vortex Cooled Air Vest: Air cooling system that covers trunk. A commercially available vest designed to distribute cooled air from a vortex tube around the torso was tested. The vest was worn over a tee shirt. It was feed by an air compressor at 85 psi. the weight of the vest was 0.52 kg.

- Ice Vest: ice cooling garment that was donned over the head and closed around the torso by two straps on each side. The vest is made of heavy cotton with a layer of Thinsulate® insulation against outside heat. There were three horizontal pockets on the front and back that contained the ice in a water-gel form. The ice vest weighted about 0.7 kg empty and 5.2 kg fully charged.

USF Experiment Measurements

Rectal temperature was measured with a thermistor that was inserted 10 *cm* beyond anal sphincter. Heart rate was monitored from a three-lead EKG system and strip chart. Metabolic rate was measured using a dry gas meter to measure the expired air volume, and to collect a sample of expired air for oxygen analysis. The experiment stopped whenever the recorded rectal temperature reached 38.5°C, or heart rate reached 90% of the allowed maximum rate (approx. 170), or any untoward symptom appeared.

USF Experiment Subjects

Eleven subjects, four women and seven men, were recruited for the experiments. The physical characteristics of each subject such as gender, height, weight and age, are showed in Table D1, APPENDIX D.

Comparisons of Simulation Results with USF Experiment Data

Computer simulations are carried out for water/air/ice cooling under similar conditions, including controls without cooling, water cooling suit, water cooling jacket, water cooling vest, air vest cooling and ice vest cooling. For each set of comparison, the transient trunk core temperatures are compared under similar conditions. For the experiment, core temperature was represented by rectal temperature.

In the thermoregulatory model employed in our model, we set the initial trunk core temperature to 36.8 °C. However, in USF experiments, the initial temperatures were normally 37.2~38°C. This might due to those subjects were preparing for the experiment or not staying still in a comfortable environment. To meet this initial condition, the simulation runs first with original initial condition as prescribed in the thermoregulatory model with a low metabolic rate at 90 W, which is very close to the basal metabolic rate. When the trunk core temperature reached the correspondent experiment initial condition, the metabolic rate is then set to the required value according to experiment data and cooling is then turned on if any.

Control-without Cooling

Figure 4.1 shows the simulation result and experiment data for control case (without any cooling system) of subject A. The simulation was based on subject A initial trunk core

temperature, metabolic rate, weight and height. The metabolic rate is 280 W. The simulation result is acceptable compared with the experiment data.

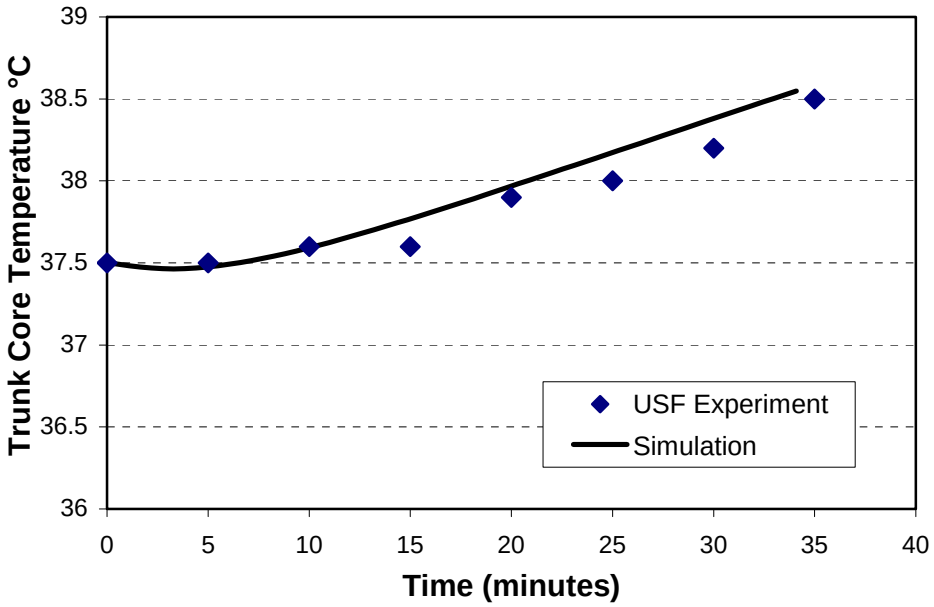

Figure 4.1 Comparison on Control without Cooling between Simulation and USF Experiment—Subject A (M=280 W)

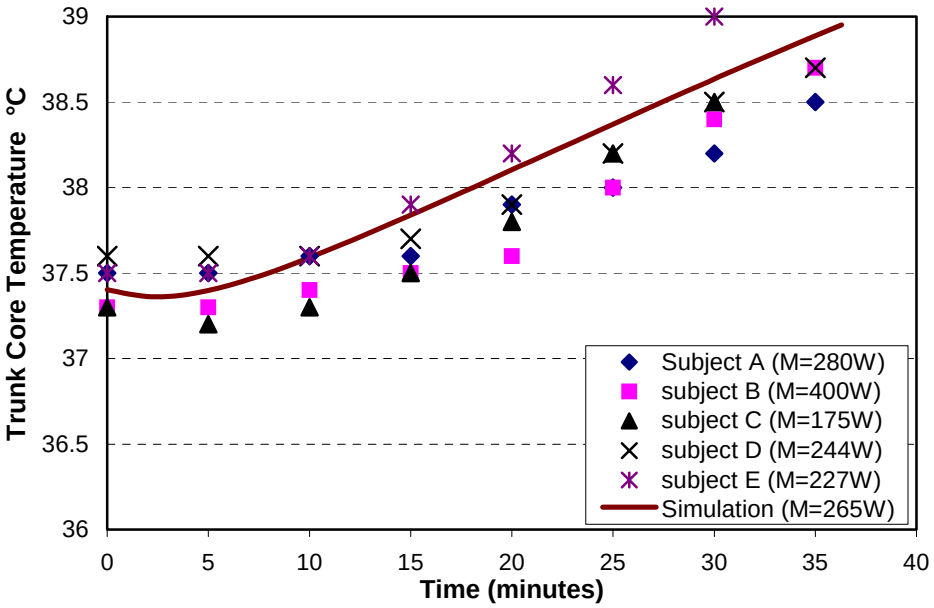

Figure 4.2 Comparison on Control (No cooling) between Simulation and USF Experiment

It may not be practical to predict each individual subject in real life. Group prediction is preferred to provide an approximately exposure time without heat stress. Figure 4.2 shows the experiment data for all five subjects. All subjects had different initial trunk core temperature, metabolic rate, height and weight. The simulation was based on a standard man (a height of 1.72 m, a weight of 74.4 kg, with 15% fat, volume of 74.4×10^{-3} m^3, and surface area of 1.89 m^2) with averaged experimental initial core temperature (37.4°C) and metabolic rate (265 W). The predicted allowable exposure time is 27.5 minutes, while subject E giving the shortest time of 24 minutes and subject A giving the longest time of 35 minutes.

Water Cooling

For water cooling system, the circulated cool water extracted heat from human body, and was re-cooled when flowing through a heat sink with ice. The temperature of the heat sink was monitored and the ice was replaced when the heat sink temperature reached 10°C. the individual simulation results and group prediction results are showed in Figure 4.3 to Figure 4.8. All individual simulations were based on individual initial trunk core temperature, metabolic rate, height and weight. For group predictions, the simulation was based on standard man with average metabolic rate and average initial trunk core temperature.

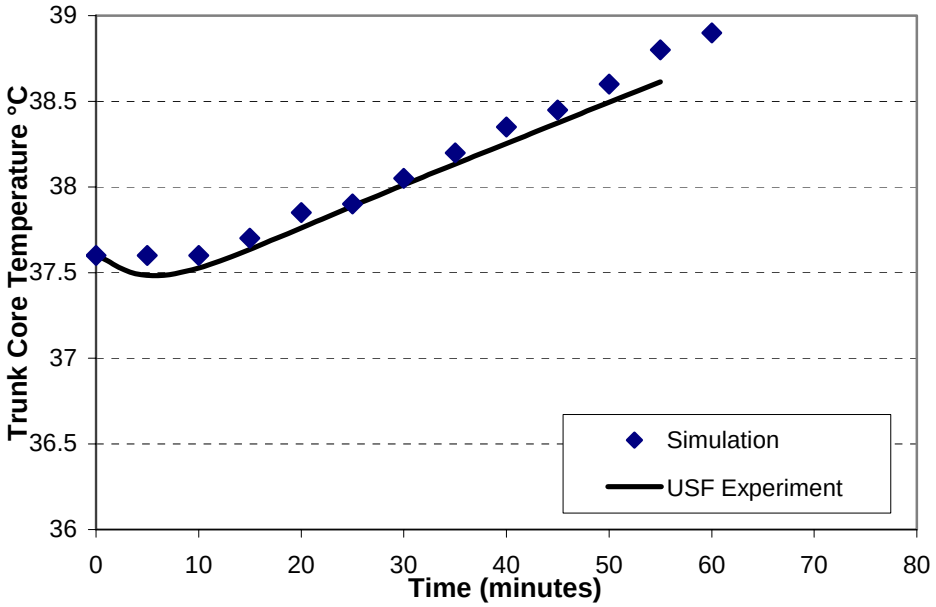

Figure 4.3 Comparison on Water Cooling Vest between Simulation and USF Experiment—Subject A (M=318 W)

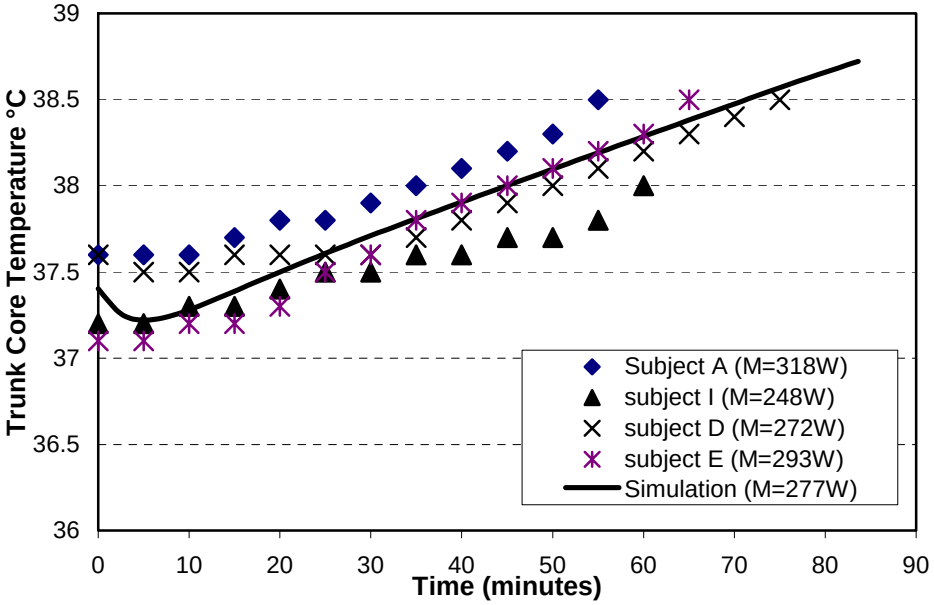

Figure 4.4 Comparison on Liquid Cooling Vest between Simulation and USF Experiment

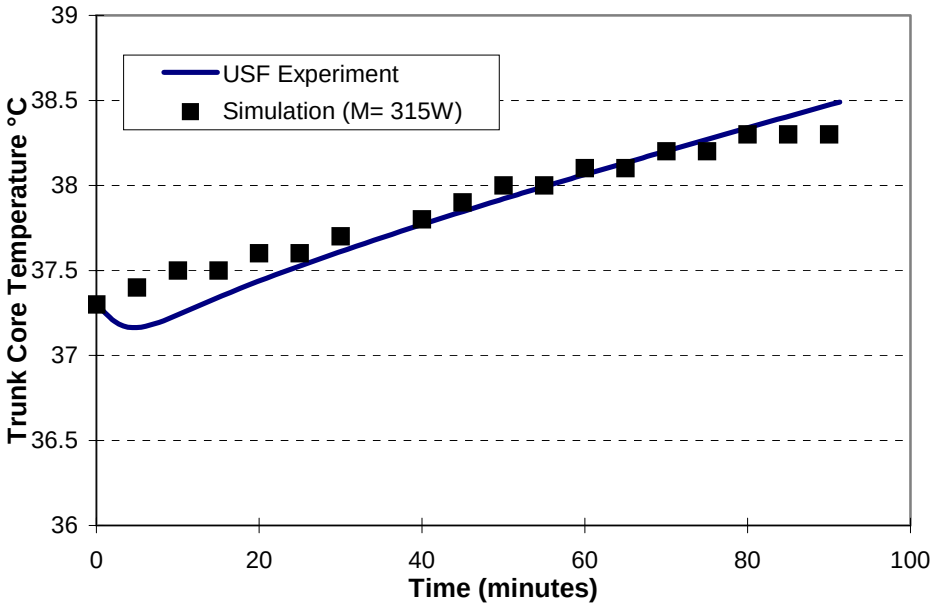

Figure 4.5 Comparison on Water Cooling Jacket between Simulation and USF Experiment—Subject A (M=315 W)

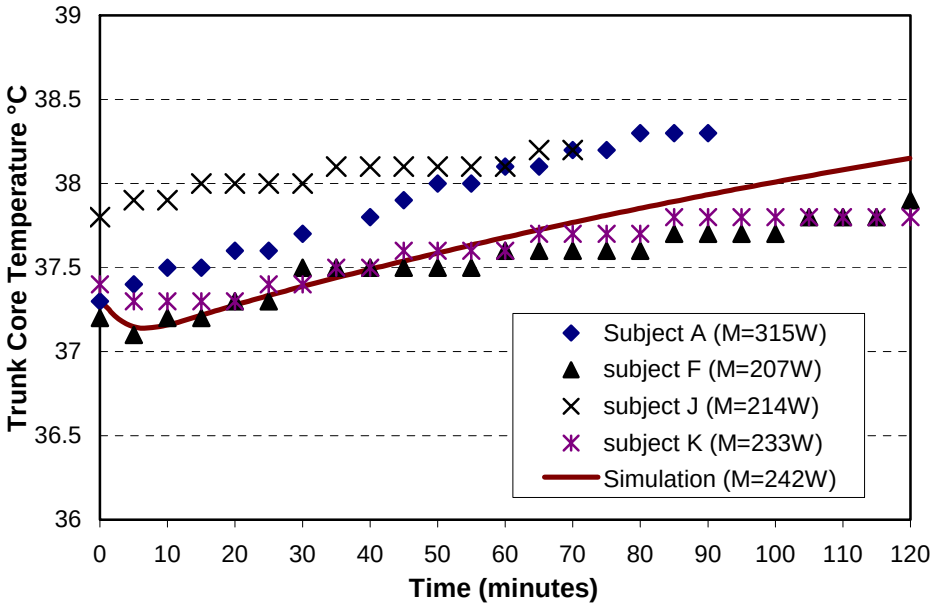

Figure 4.6 Comparison on Water Cooling Jacket between Simulation and USF Experiment

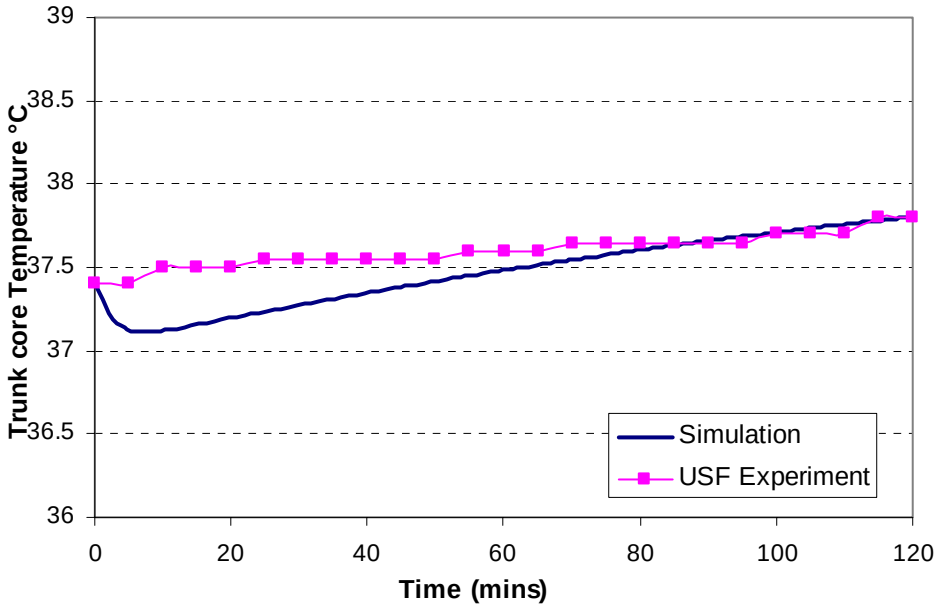

Figure 4.7 Comparison on Water Cooling Suit between Simulation and USF Experiment—Subject A (M=277 W)

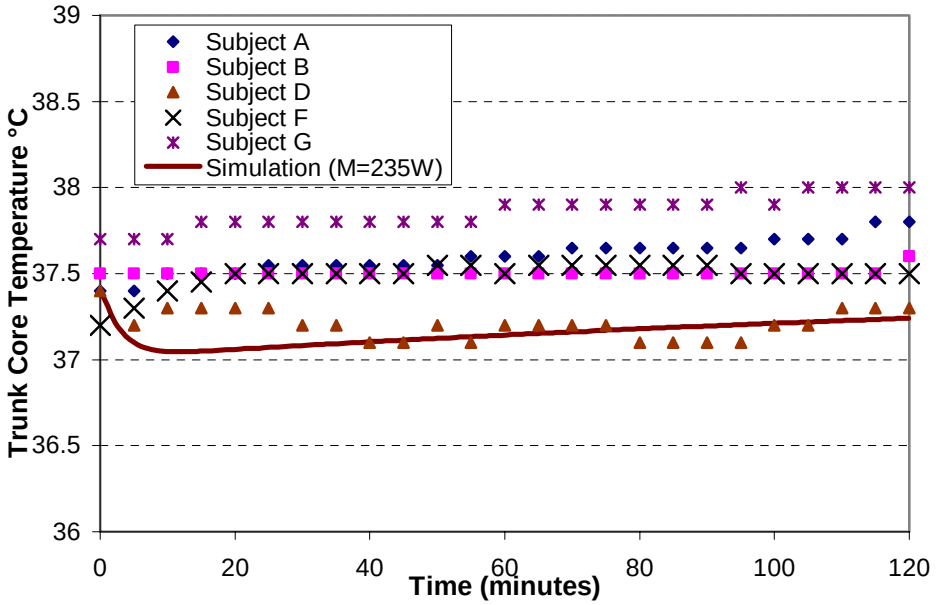

Figure 4.8 Comparison on Water Cooling Suit between Simulation and USF Experiment

The simulation results give a good prediction of the exposure time except for liquid cooling suit due to too much temperature drop at the first five minutes. This issue will be discussed later.

Air Cooling

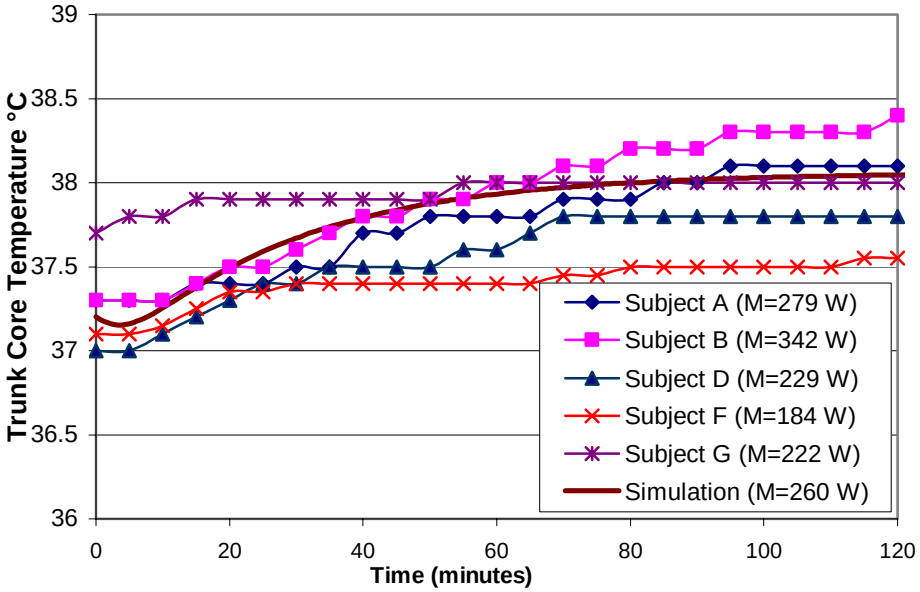

Figure 4.9 Comparison on Air Cooling Vest between Simulation and USF Experiment

Figure 4.9 shows the USF experimental data on the air cooling vest. Five subjects participated in the experiments. The average metabolic rate is about 260 *W*. The five subjects have different weights, heights, initial core temperatures and metabolic rates. Practically it's more useful to do a group prediction than to simulate individual subject. Simulation result of standard man with a metabolic rate of 260 *W* is also showed in the figure. The inlet cooling air temperature used in the simulation is 10°C, and relative

humidity is 80%. The inlet mass flow rate of the cooling air is 10 CFM. Similar with water cooling simulation, the agreement between model prediction and USF experiment is acceptable except that there is a fall in trunk core temperature predicted by the model at the time the cooling air is switched on.

Ice Cooling

Figure 4.10 shows the comparison between USF experimental data and simulation result, the metabolic rate is 260 *W,* which is the average metabolic rate of all subjects. The exposure time for different subjects varies a lot.

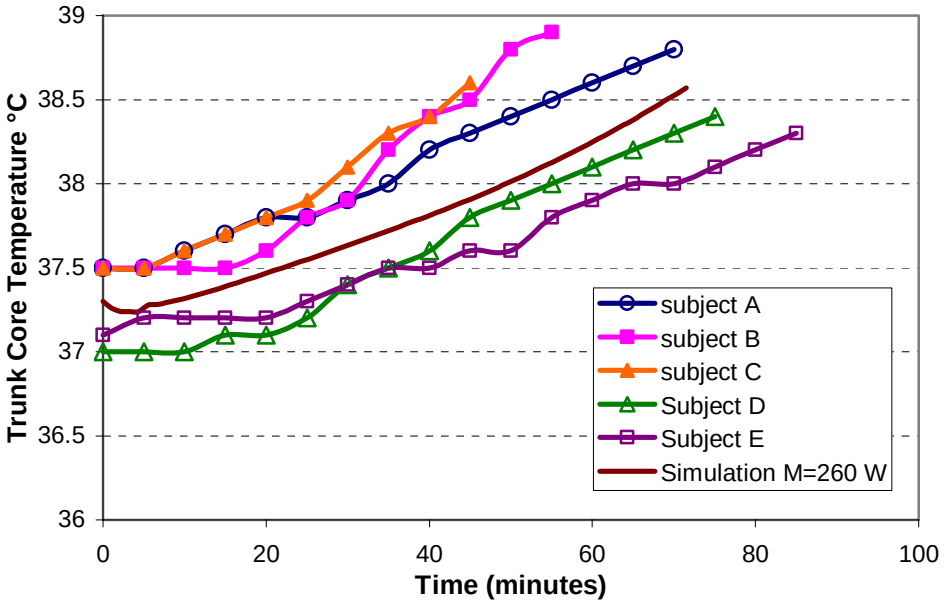

Figure 4.10 Comparison on Ice Cooling Vest between Simulation and USF Experiment

Model Limitations

From above simulation results, the agreement between model prediction and USF experiment is acceptable except for the rather large fall in trunk core temperature predicted by the model at the time the cooling system is switched on.

$$Q_{core} = M_{core} - E_{res} - C_{res.} - Q_{blood} - Q_{cond.} \quad (4.1)$$

Trunk core temperature change is decided by the net heat storage in trunk core which is calculated by above equation. From Stolwijk and Hardy model, $M_{core} = M_{core\_basal}$, which means the metabolic rate generated in trunk core is constant. The respiration heat loss from trunk core (E_{res} + C_{res}) is relatively small compared with other terms in the equation and it does not change much. The conduction term $Q_{cond.}$ does not change much either and the value is always negligible. However, the heat related to blood Q_{blood} experiences a sudden change. Q_{blood} is related to trunk core blood flow rate and temperature difference between trunk core and blood. As Stolwijk mentioned, the blood flow rate of the trunk core is almost constant no matter how large metabolic rate is. It is clear now that the sudden change of Q_{blood} results from blood temperature change which is partly due to the sudden change of skin temperature.

It is noted that, in the computer simulation this happens only within the first five minutes. Once the thermoregulatory control system senses the drop of core temperature and skin temperature, commands are sent out to make the blood vessels constrict, resulting

in less blood flow. Furthermore, the temperature difference between the cooling water and the skin also decreases. Therefore, the trunk core temperature then increases gradually. Yan (2002) concluded that the temperature drop resulted from skin temperature when the cooling was applied by analyzing the heat balance of trunk core.

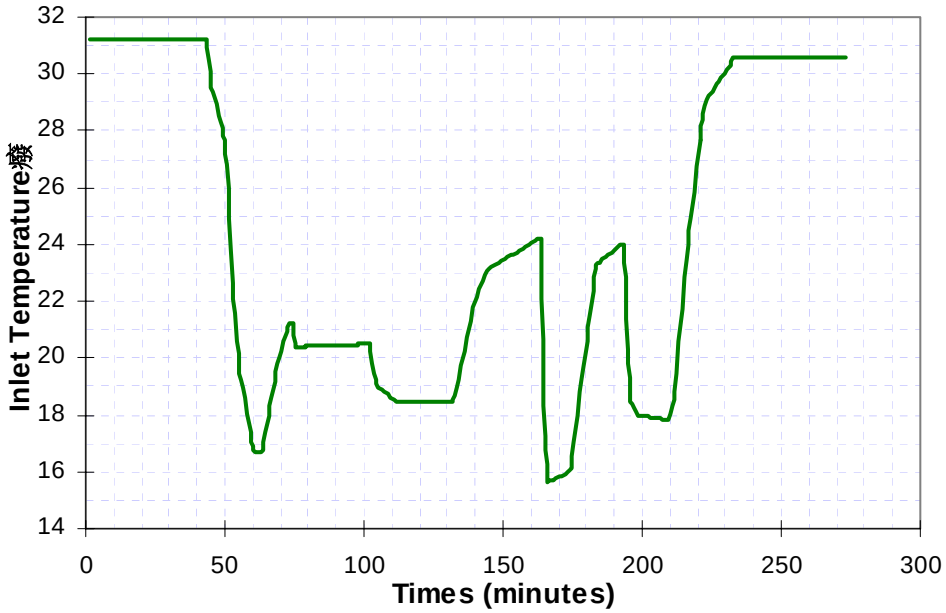

Figure 4.11 Cooling Water Inlet Temperature

Sudden skin temperature drop may not be the only reason. It is noticed that there is a temperature drop even without cooling applied when there is a metabolic rate jump. Metabolic rate jump may be another reason for the temperature jump. Simulation with changing metabolic rate is carried out based on the water cooling suit. The water inlet temperature is showed in Figure 4.11. Metabolic rate and trunk core temperature are showed in Figure 4.12. The cooling water was first supplied at time 43 minutes and the metabolic rate start jumping at time 40 minutes. The results show the trunk core

temperature starts to drop even before the cooling is applied. The heat balance of trunk core was analyzed and the results are showed in Figure 4.13. As expected, the blood heat transfer plays a big role in the trunk core temperature.

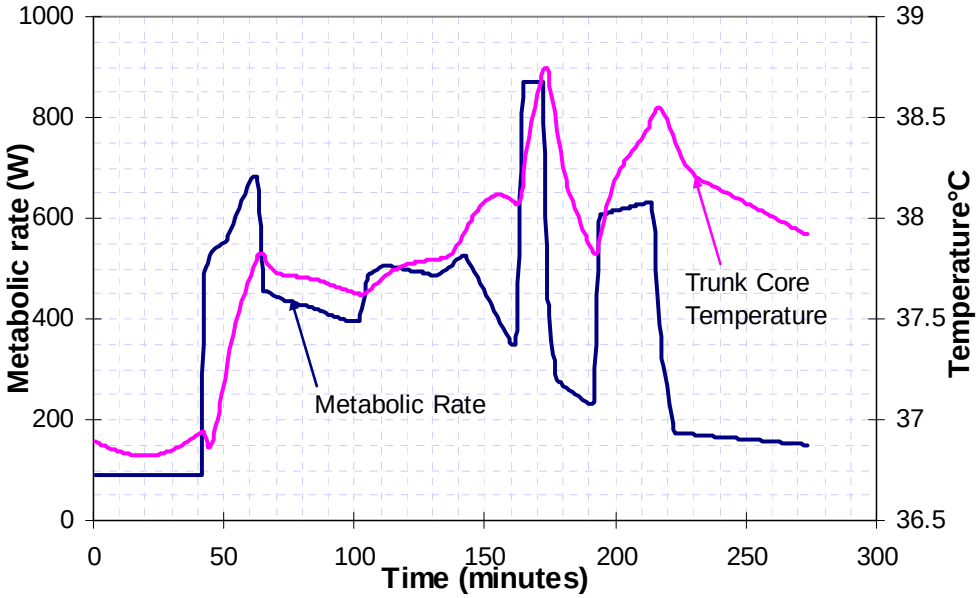

Figure 4.12 Trunk Core Temperature and Metabolic rate

Blood heat transfer in trunk core is decided by the temperature difference between trunk core and blood. Figure 4.14 shows the temperature of trunk core, blood, trunk muscle and leg muscle. After carefully analyses of the simulation results, it shows that metabolic rate jumping is a big contributor for the sudden blood temperature drop which is shown in Figure 4.14. The metabolic rate jump increases the muscle blood flow rate dramatically, as showed in Figure 4.15. Since the muscle temperature is lower than blood temperature, it takes a lot of heat from blood when the metabolic rate jumps, which makes the blood temperature drop dramatically.

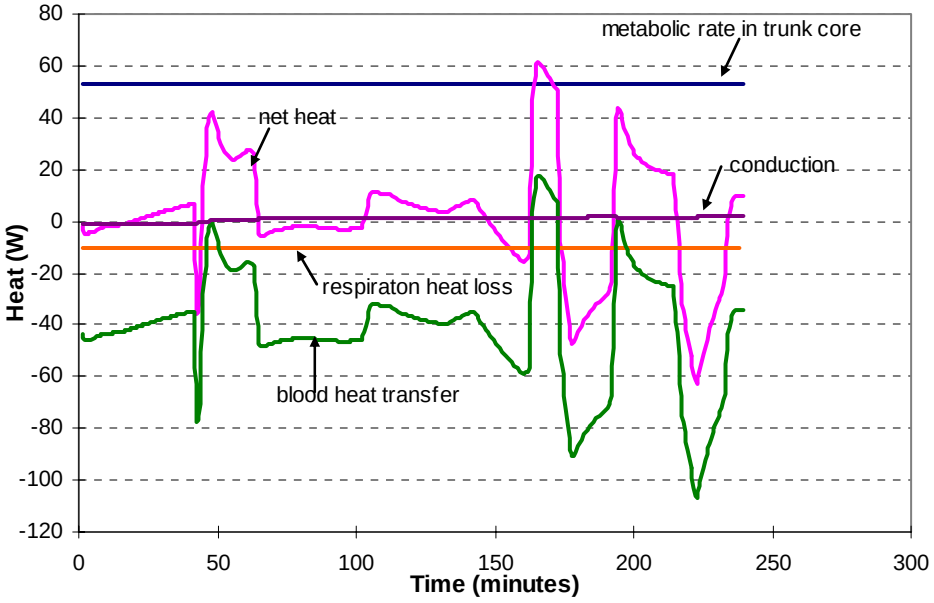

Figure 4.13 Heat Balance in Trunk Core

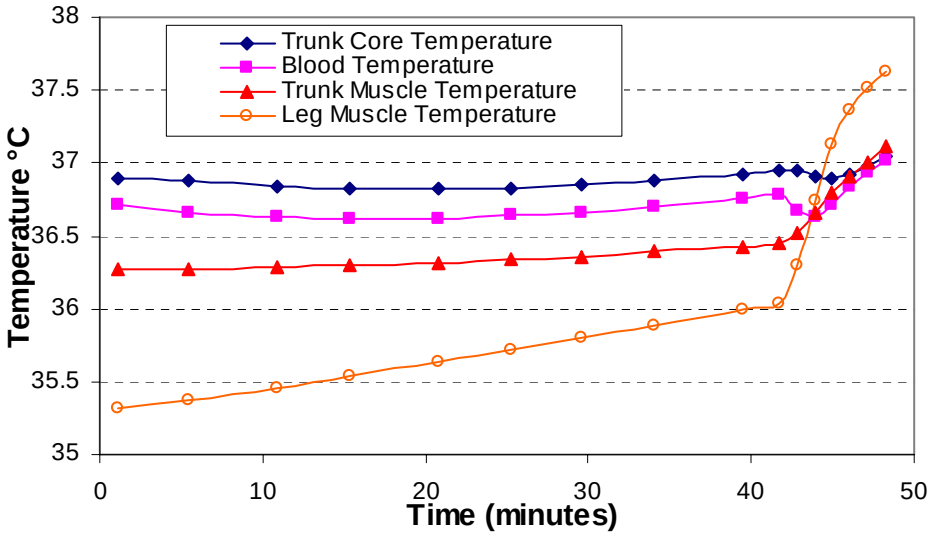

Figure 4.14 Temperatures for Trunk Core, Blood, Trunk Muscle and Leg Muscle

The temperature drop of trunk core is not practical since such drop is not noticed in the experiment data. It may result from inappropriate assumptions of the thermoregulatory model. First, the model representation of peripheral blood flow does not allow sufficient rapid vasoconstriction during the cooling of the skin, so the blood loses more heat than expected. Second, in the thermoregulatory model, the blood temperature leaving a body part is assumed to be the same of that body part. It is true for most cases, but it may not be right when the blood flow rate surges, large blood vessels in the trunk have relatively little heat transfer with surrounding tissues due to the high blood flow rates and incomplete contact with tissues (Chato 1980; Chen and Homes 1980). Stolwijk also noticed the incorrect rapid and transient drop in trunk core temperature at the onset of exercise predicted by the thermoregulatory model. Stolwijk suggested combining the thermoregulatory model with simultaneous models of cardiovascular and the respiratory system to get a more realistic model.

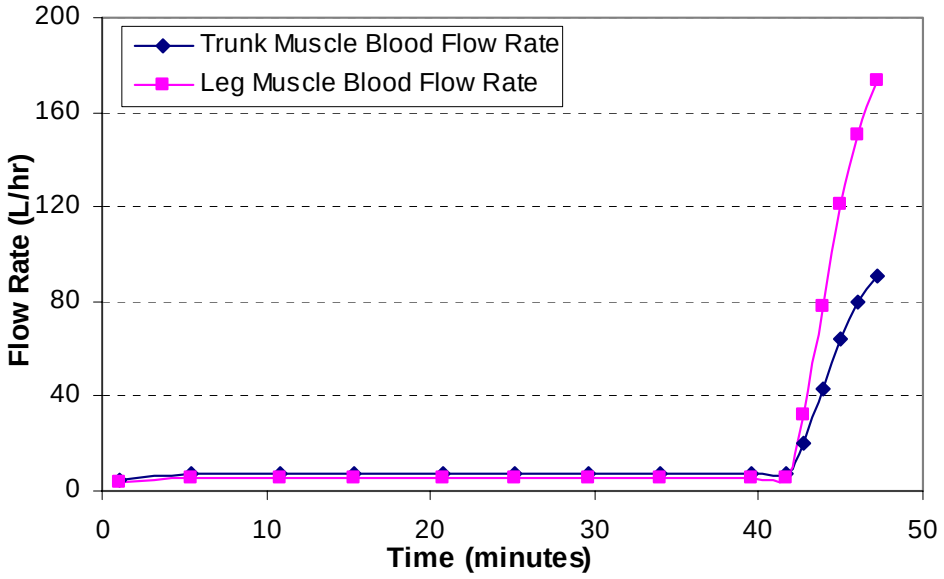

Figure 4.15 Trunk and Leg Muscle Blood Flow Rate

The thermal model presented in this dissertation can provide a reasonable prediction of human response when the metabolic rate keeps constant. It does not function well when metabolic rate changes very fast and dramatically due to the incorrect assumption of thermoregulatory model.

CHAPTER 5 APPLICATIONS

Metabolic rate is the most important factor, which affects human body thermoregulatory response. There are also other factors which play an important role. Such as environment condition, PPE property, clothing properties, cooling water/air inlet temperature and cooling water/air flow rate. It is impractical to study the physiological responses of a person wearing PPE with personal cooling experimentally due to too many factors involved. The thermal model presented a way to understand how these factors affect human body thermoregulatory response.

Applications to PPE

Comparison with Water Cooling Lumped Model

Figure 5.1 shows the trunk core temperature and accumulated heat removal predicted by both lumped model and our thermal model; both predictions are under exact same conditions (metabolic rate, cooling water inlet temperature thermal resistance and environment temperature). However, lumped model always over predicts the heat removal from human body, which results in a much lower trunk core temperature. The over prediction is due to the larger temperature difference between human body and cooling water predicted by the lumped model because it considers the whole body as a

uniform temperature node. The actual human body temperature distribution is non-uniform especially when personal cooling is applied. The skin temperature predicted by the thermal model was much lower than the average body temperature. The whole comparison shows that a lumped model cannot provide a reasonable prediction of the body temperature.

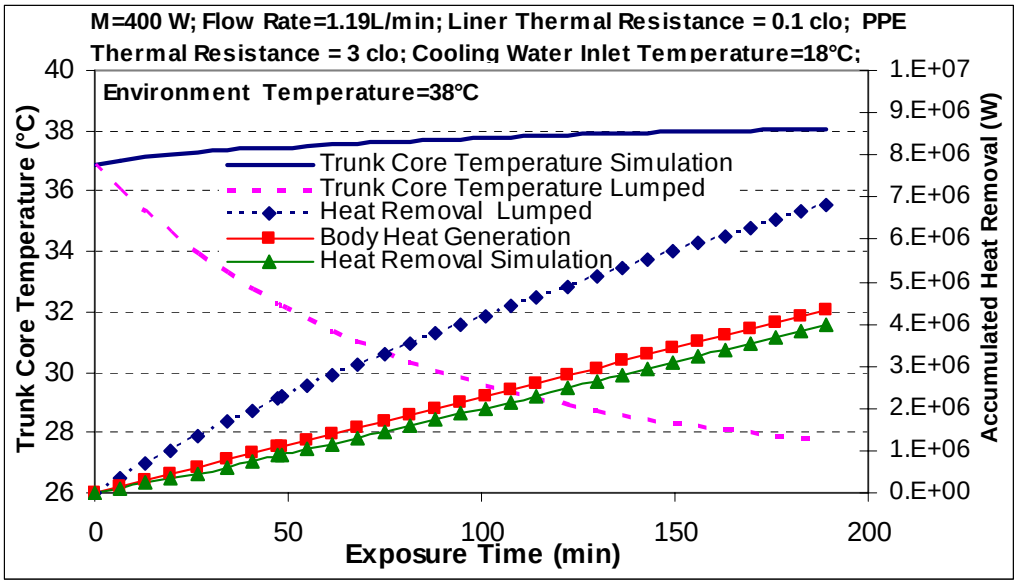

Figure 5.1 Comparisons of Trunk Core Temperature and Accumulated Heat Removal Predicted by Lumped Model and Thermal Model

Water Cooling Parametric Study

To show how the human body can benefit from personal liquid cooling garment, simulation results for control case are first presented in Figure 5.2. Figure 5.2 shows the trunk core temperature predicted by thermal model for human body with no personal cooling under various metabolic rates. The environment temperature is 38ºC; the

thermal resistances of PPE and liner are 3clo (1clo = 0.155 m^2K/W) and 0.1clo, respectively. Heat stress limit is assumed to occur when the trunk core temperature reaches 38.5ºC. The results show the maximum exposure time changes from 19 minutes to 33 minutes then the metabolic rate decreases from 500 W to 300 W.

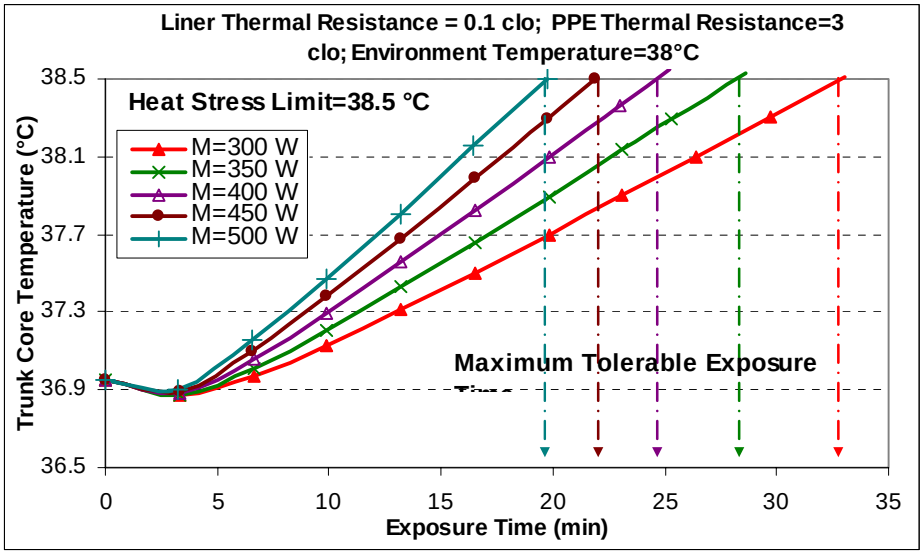

Figure 5.2 Trunk Core Temperature vs. Metabolic Rate without Personal Cooling

To see how metabolic rate, clothing properties, cooling water inlet temperature and flow rate affect the human body thermoregulatory responses, several different group simulations were done and the simulations results are showed in Figure 5.2-Figure 5.8.

Figure 5.3 shows the simulation results for different metabolic rates. In the simulation, the cooling water inlet temperature is fixed at 20ºC; the cooling water flow rate is fixed at 1.19 L/min; the thermal resistances of liner and PPE are assumed to be 0.1clo and 3clo,

respectively; and the environment temperature is 38ºC. It is obvious that liquid cooling provides an extended exposure time compared with control case showed in Figure 5.2. It is noted that metabolic rate has a great effect on the maximum exposure time (stress limit is 38.5ºC).

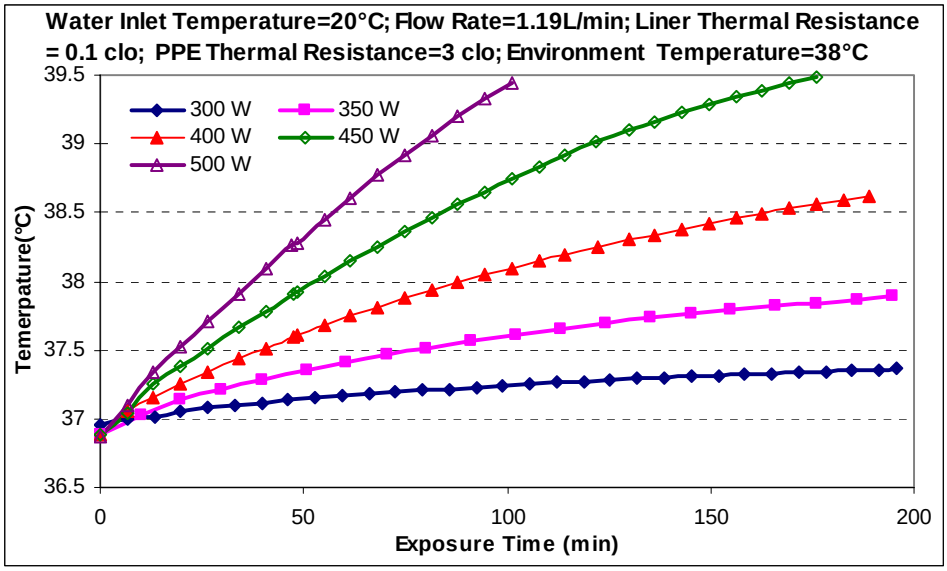

Figure 5.3 Trunk Core Temperature vs. Metabolic Rate with Liquid Cooling Garment

Figure 5.5 presents the simulation results with various cooling water inlet temperatures. The lower water inlet temperature provides a larger temperature difference between skin and cooling water, so more heat is removed from human body. But too low an inlet temperature may result in low skin temperature, which may lead to local discomfort.

Figure 5.4 shows the maximum exposure time with various liner thermal resistance and cooling water inlet temperature. The liner resistance is an important factor in the heat removal from the skin. The smaller the resistance, the more heat will be removed from

human body, which will result in longer exposure time. Skin temperature is also affected by the liner resistance. Too small a liner thermal resistance may result in a low skin temperature which may lead to local discomfort.

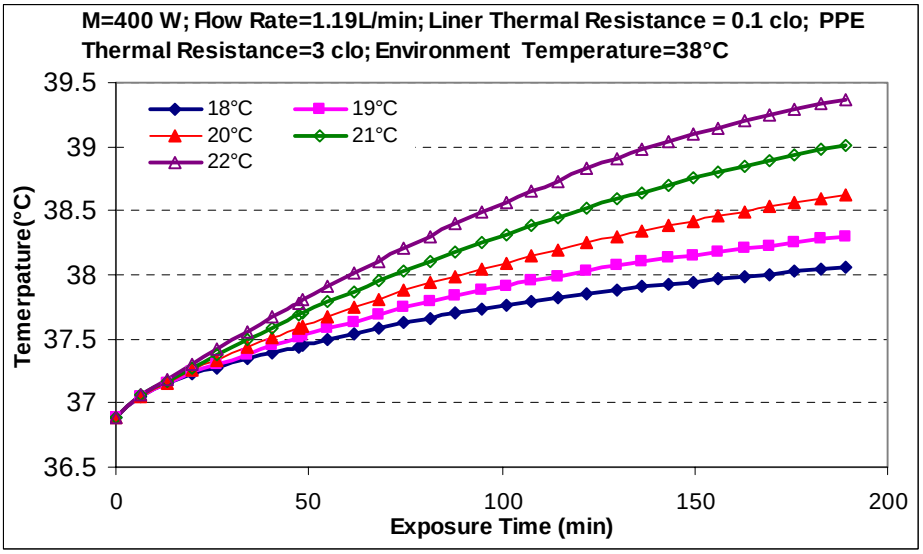

Figure 5.5 Trunk Core Temperature vs. Cooling Water Inlet Temperature

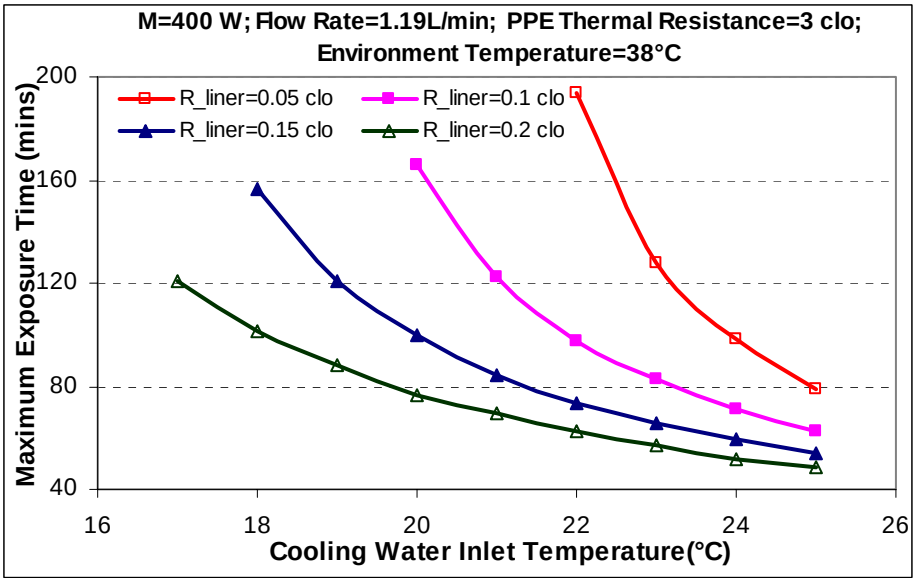

Figure 5.4 Maximum Exposure Time under Various Liner Thermal Resistance and Cooling Water Inlet Temperature

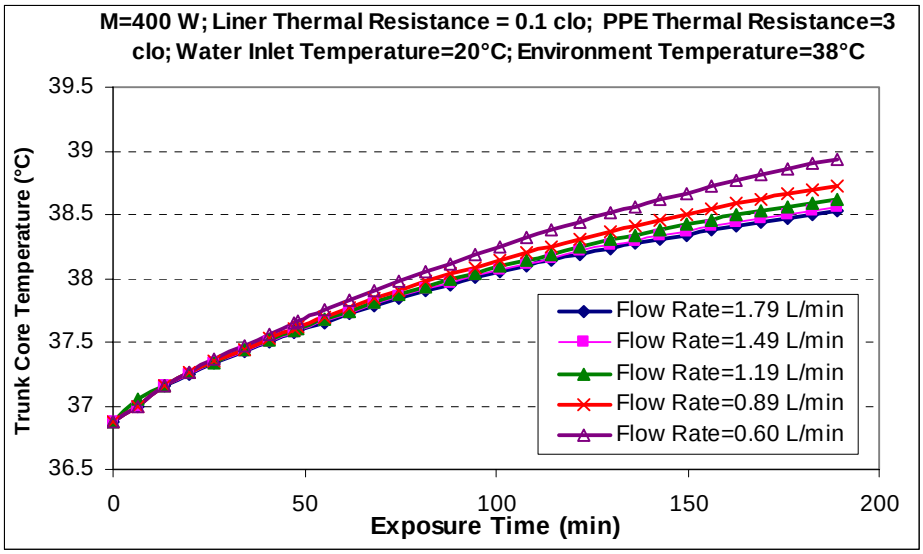

Figure 5.6 Trunk Core Temperature vs. Cooling Water Flow Rate

Figure 5.6 presents the trunk core temperature with different cooling water flow rate. The results show that the cooling water flow rate does not have a large effect on the trunk core temperature. In other words, the increased cooling water flow rate cannot remove much more heat from the human body because the overall heat resistance between the cooling water and the human body skin is dominated by the water tube and liner resistances.

Figure 5.7 shows the trunk core temperatures with various PPE resistances. The PPE resistance is relatively large and there is only very small amount heat transfer occurring between the environment and the human body compared to the heat removal by the cooling water. The simulation results show that PPE thermal resistance does not have a significant effect on the human thermoregulatory response.

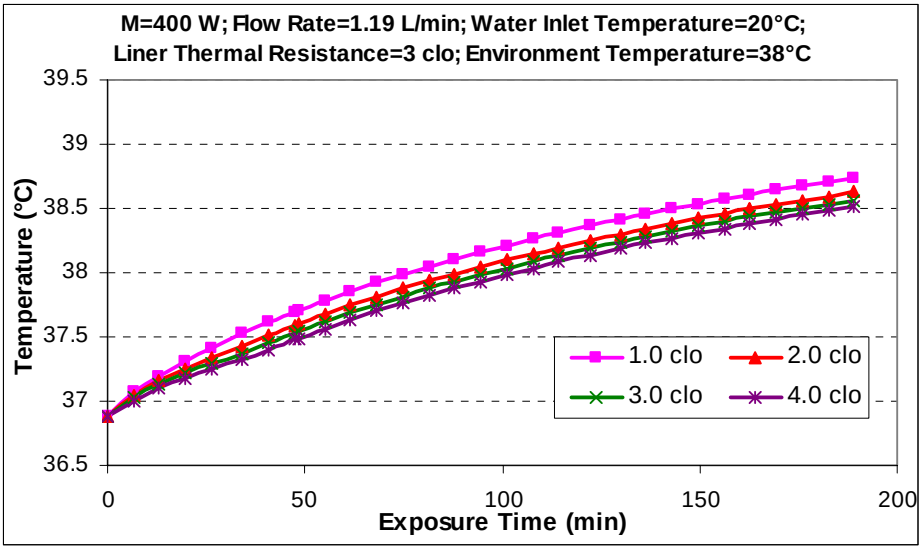

Figure 5.7 Trunk Core Temperature vs. PPE Thermal Resistance

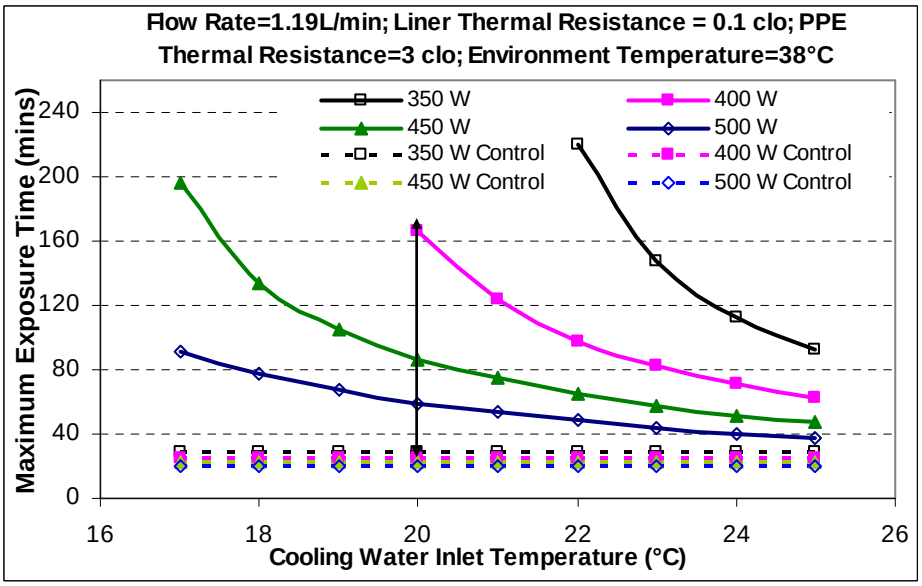

Figure 5.8 Maximum Exposure Time under Various Metabolic Rate and Cooling Water Inlet Temperature

Figure 5.8 shows the maximum exposure time under various metabolic rate and cooling water inlet temperature. The dotted lines represent the maximum exposure time for

control cases (no personal cooling). The difference between the solid line and dotted line shows the gained exposure time with the liquid cooling garment. The figure is especially useful when choosing a cooling system.

Air Cooling Parametric Study

Five different cases were simulated with metabolic rates of 220 W, 260 W, 300 W, 400 W and 500 W to see the different trunk core temperature responses. Figure 5.9 shows the simulation results. As depicted in the figure for high metabolic activities (>400 W), the exposure time decreases as the metabolic rate increases. The air cooling garment is not able to provide sufficient cooling to wearer with a high metabolic rate.

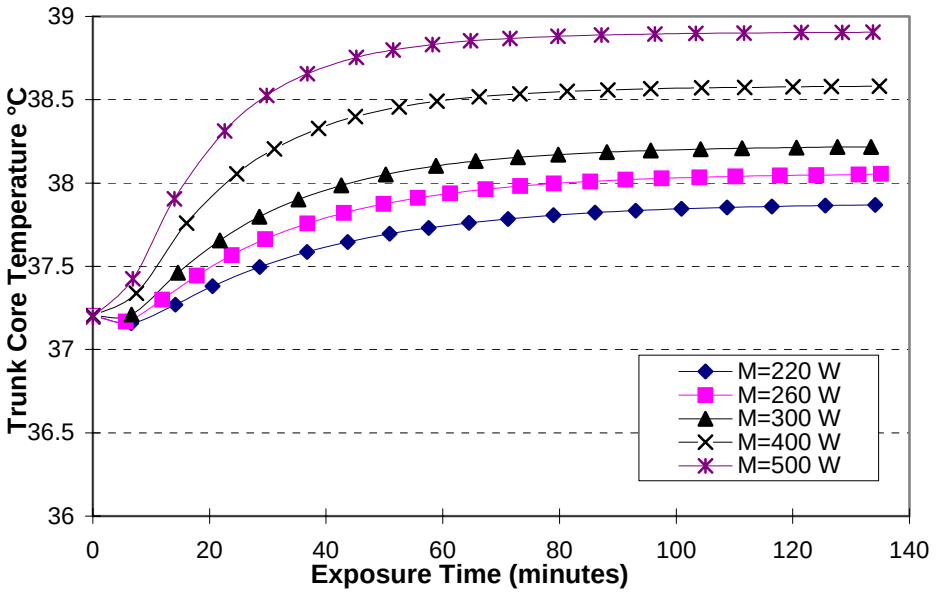

Figure 5.9 Trunk Core Temperature vs. Metabolic Rates (Cooling Air Flow Rate=10 CFM; Inlet Temperature=10°C)

Metabolic rate is the most important factor, which affects human body thermoregulatory response. There are also some other factors which also play an important role. To see how the cooling air inlet temperature, relative humidity and flow rate affect the human body thermoregulatory responses, several different group simulations were done and the simulations results are showed in Figure 5.10, Figure 5.11 and Figure 5.12.

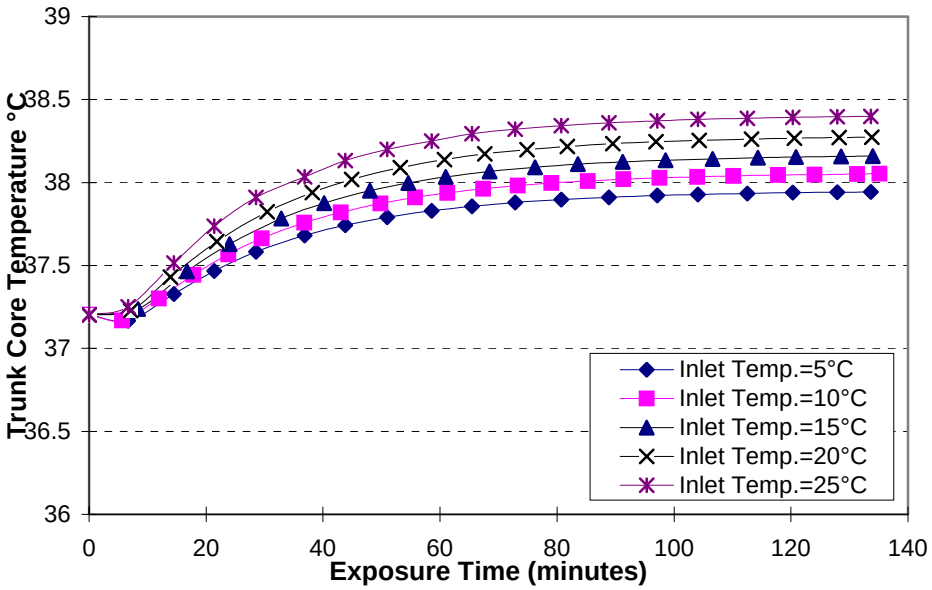

Figure 5.10 Trunk Core Temperature vs. Inlet Cooling Air Temperature (M=260W, Cooling Air Flow Rate=10 CFM)

Figure 5.10 presents the simulation results with various inlet cooling air temperatures. The lower the inlet temperature, the better the cooling effect. But too low inlet temperature may result in overly low skin temperature, which may lead to local discomfort.

Figure 5.11 shows the simulation results with different cooling air flow rate. In the simulation, the metabolic rate is fixed at 260 W; the cooling air inlet temperature is fixed at 10°C; the relative humidity of the inlet cooling air is 80%. shows that the higher the flow rate, the better the cooling effect. It is noticed that increasing the flow rate provides a great cooling effect.

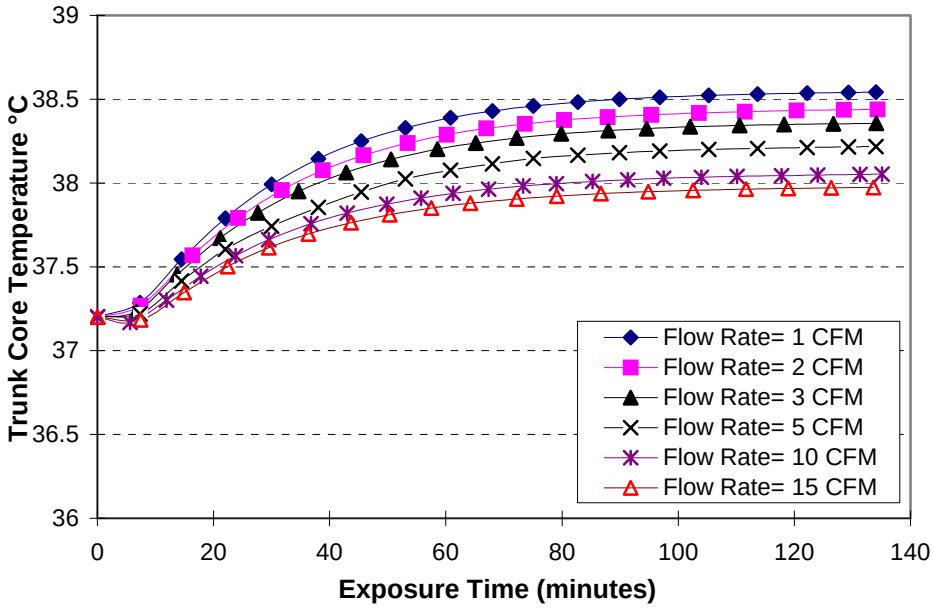

Figure 5.11 Trunk Core Temperature vs. Inlet Cooling Air Flow Rate (M=260W; Cooling Air Inlet Temperature=10°C)

Figure 5.12 shows the simulation results with various relative humidity at two different metabolic rates. For a metabolic rate of 260 W, there is slightly noticeable difference among simulation results with various relative humidity. For a metabolic rate of 500 W, there is a distinct difference between the simulation results (50%, 80% and 95%). Evaporative heat removal is the dominant heat transfer factor in the air cooling garment,

most heat generated by metabolic rate is removed by evaporating sweat. For low metabolic rate (260w) activity, the sweat is limited and it can be totally removed by the cooling air, even if the inlet cooling air relative humidity as high as 95%. However, for a high metabolic rate (500w) activity, the sweat generated is much more, the sweat may not be able to be removed by the cooling air if the relative humidity of inlet cooling air is too high (95%).

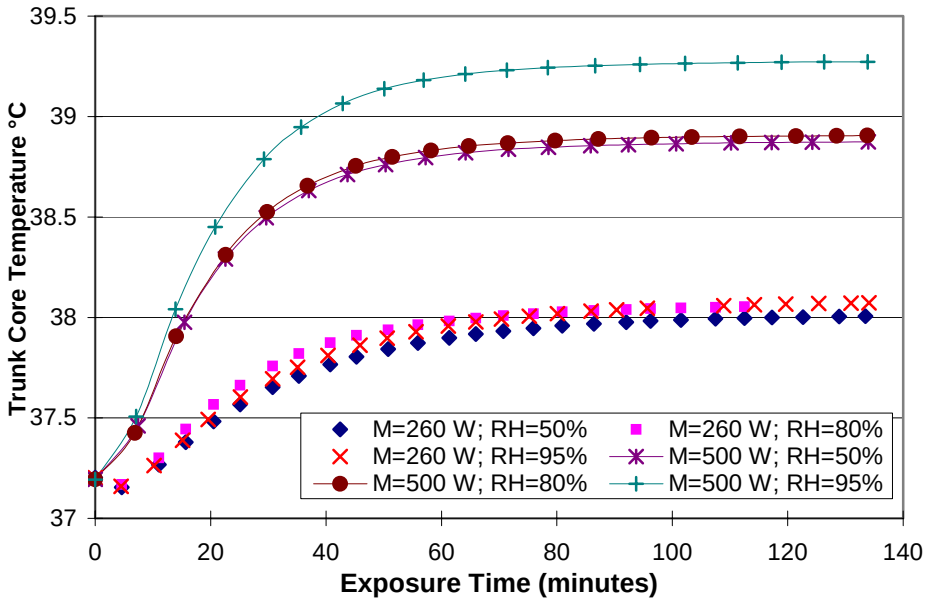

Figure 5.12 Trunk Core Temperature vs. Inlet Cooling Air Relative Humidity (Inlet Cooling Air Temperature = 10°C)

Figure 5.13 shows the simulation results with various T-shirt heat resistances. The inlet cooling air temperature used in the simulation is 10°C, and relative humidity is 80%. The inlet mass flow rate of the cooling air is 10 CFM. Metabolic rate is 260 W. As expected, the lower the heat resistance, the better the cooling effect.

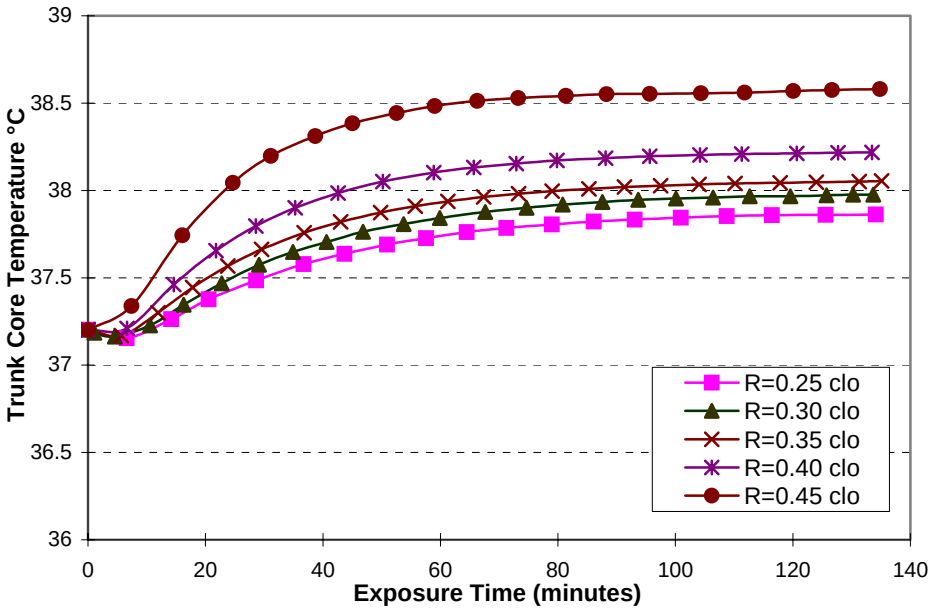

Figure 5.13 Trunk Core Temperature vs. Heat Resistance of T-shirt

Application To Extra-Vehicular Activities

Extra-vehicular activities (EVA) on Mars require suits with sophisticated thermal control systems so that astronauts can work comfortably for extended periods of time. The Extravehicular Mobility Unit (EMU), commonly called a space suit, is a self-contained environment for astronauts. Besides protection from the elements, EMUs provide temperature control and ventilation with a one-piece mesh spandex undergarment. Water cooling tubes run through it to keep the astronaut comfortable while working in space. The current space suit is designed for the near-zero-gravity environment of

space outside the Space Shuttle and International Space Station. In deeper space, such as a journey to Mars, the demands placed on a suit would be very different from what astronauts experience now in low-Earth orbit (LEO).

Thermal Environment On Mars

From summer to winter, from equatorial regions to higher latitudes, and from night to day, there is a large variation in ambient Martian temperatures. Three different environment conditions are considered in this dissertation, one is at Ls253 deg., 8S-75W (hot case), where the atmospheric temperatures vary from –155 °F (169 K) to a maximum of 80 °F (300 K) and then down to 20 °F (267 K) during the daylight hours (6 hours to 19 hours of the Martian day at that location at perihelion); The other one is at Ls90 deg., 8S-75W (nominal cold case), where the atmospheric temperatures vary from –166 °F (163 K) to a maximum of -32 °F (237 K) and then down to -37 °F (234 K) during the daylight hours. Since this dissertation concentrates on cooling, daylight time, namely from 6 hours to 19 hours, is considered here. For the purpose of the thermal model presented here, the wind speed is taken to be 20 m/s for the hot case and 10m/s for the nominal cold case, which is quite typical at these locations.

Figure 5.14 shows the incident solar flux on a spacesuit on Mars for both the hot case and the nominal cold case. Ambient temperature and suit sink temperature are showed

in Figure 5.15 and Figure 5.16. All the figures are the data from Iovine and Horton (1999).

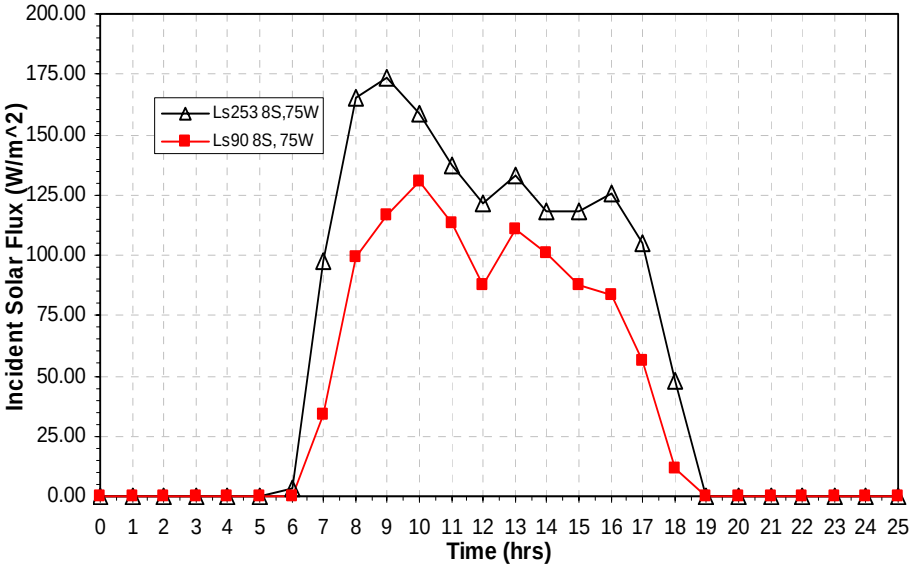

Figure 5.14 Solar insolation Diurnal Mars

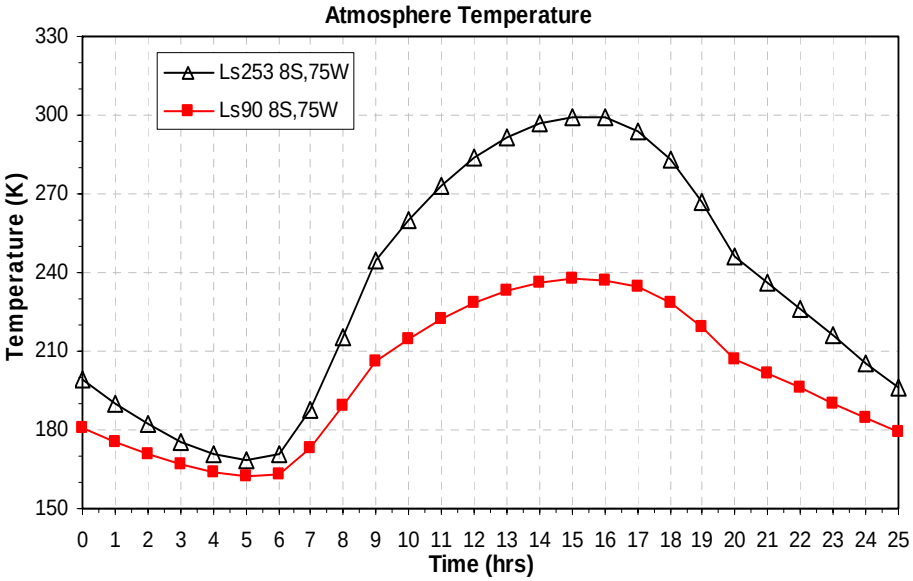

Figure 5.15 Temperature on Mars Atmosphere

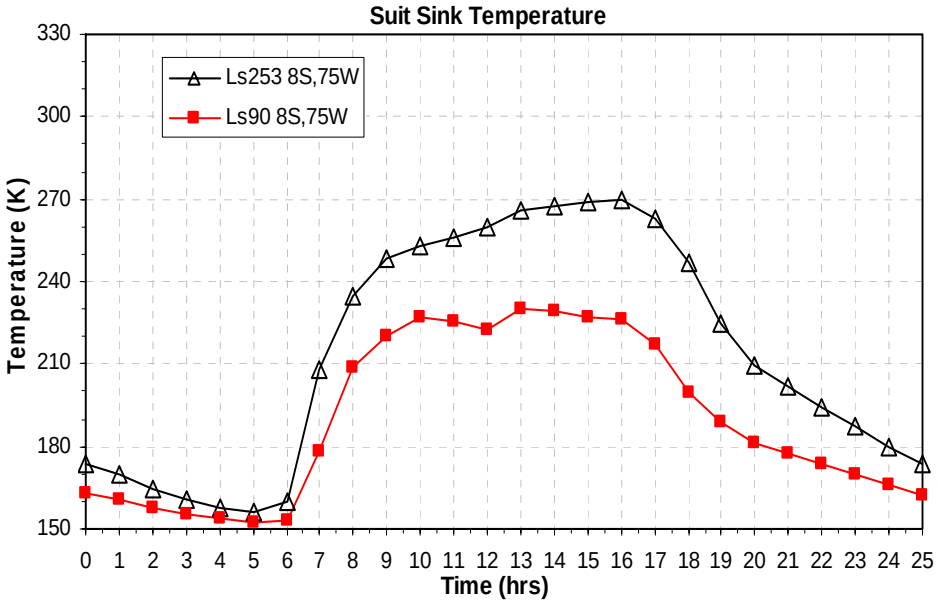

Figure 5.16 Suit Sink Temperature on Mars

Heat Transfer between the Human Body and Ambient

For the thermal analysis, metabolic rates of 275 W are considered in this dissertation. It should be noted that walking at 1.2 m/s corresponds to a metabolic rate of 275 W on earth for a “standard” person, whereas handling 50 kg bags would correspond to 440 W. The presence of gravity, though lower than what is on earth, makes the metabolic workloads higher than what they are in LEO. The heat acquisition process is assumed to be the same as that in the EMU. For the current analyses, all the heat loss is

assumed to be sensible heat loss from the body and sweat evaporation heat loss is considered to be negligible.

Radiation

Radiation heat transfer includes two parts, heat absorption and heat emission. The absorbed thermal radiation, or Q_{abs}, is that due to the net solar and infrared radiation absorbed by the outer surfaces of the space suit. Heat emission is the emitted radiation from the suit surface, or Q_{emi}.

$$Q_{abs} = (\alpha \cdot Q_{sol} + \varepsilon \cdot Q_{ir}) \cdot A_{suit} \tag{5.1}$$

$$Q_{emi} = \varepsilon \cdot \sigma \cdot A_{suit} T_{suit}^{\ 4} \tag{5.2}$$

Where Q_{sol} is solar radiation absorbed by the suit garment, Q_{ir} is infrared absorption.

Convection

Due to the low environment pressure and low atmospheric density on Mars, the convective heat transfer coefficient is much lower than that on earth at the same wind speed. The human body is considered as a vertical cylinder for convective heat transfer calculation.

$$l = \frac{\pi}{2} D \tag{5.3}$$

$$\mathrm{Re}_l = \frac{\rho u_m l}{\mu} \tag{5.4}$$

$$Nu_l = \frac{hl}{k} \tag{5.5}$$

Where D = cylinder diameter, u_m = wind speed

Over the ranges 10 < R_{el} < 107 and 0.6 < Pr < 1000, the *Nu* number can be calculated by the following equation (Gnielinski 1975)

$$Nu_l = 0.3 + \sqrt{Nu_{l,lam}^2 + Nu_{l,turb}^2} \tag{5.6}$$

where

$$Nu_{l,lam} = 0.664\sqrt{\mathrm{Re}_l}\sqrt[3]{\mathrm{Pr}} \tag{5.7}$$

$$Nu_{l,turb} = \frac{0.037\,\mathrm{Re}_l^{0.8}\,\mathrm{Pr}}{1 + 2.443\,\mathrm{Re}_l^{-0.1}(\mathrm{Pr}^{2/3} - 1)} \tag{5.8}$$

All physical properties of the environment gas used in the above calculations are based on ideal CO_2 gas with 20 °C temperature and 1.0 kPa pressure.

Conduction

The heat transfer by conduction can be solved if both the overall conductance term and the temperature difference across the space suit are known, along with the space suit area.

$$Q_c = A_{suit} \cdot \lambda \cdot \Delta T \tag{5.9}$$

The space suit area is calculated from nude body surface area and clothing surface area correction factor.

$$A_{suit} = f_c A_{nude} \tag{5.10}$$

The clothing surface area correction factor (ASHRAE 1977) has been found experimentally to be

$$f_c = 1.00 + \frac{1.27}{\lambda} \tag{5.11}$$

Pending on the selection of Mars insulation material and test results, a preliminary estimate is made to carry out the calculations. Suit insulation conductance of 0.62 W/m^2K was chosen as an analysis baseline for cold case. In a hot environment, the overall conductance is approx. twice that of the cold environment because of the temperature dependence of thermal conductivity. The Preliminary exterior surface optics of 0.5 solar absorptance and 0.8 infrared absorptance and emittance were chosen as the analysis baseline.

Simulation Results

Case 1: No Personal Cooling (hot condition 13 hours-)

The body keeps generating heat, but only a small part of heat could leak out of human body due to the high heat insulation of space suit. The environment condition is based on Mars hot case 13 hours and the metabolic rate is assumed to be 275 W in the

simulation, which is a typical number for planetary work of an astronaut. The simulation result is shown in Figure 5.17; we can see that trunk core temperature of human body with 275 W metabolic rate will increase to 38.5°C in less than 35 minutes if no personal cooling system is applied.

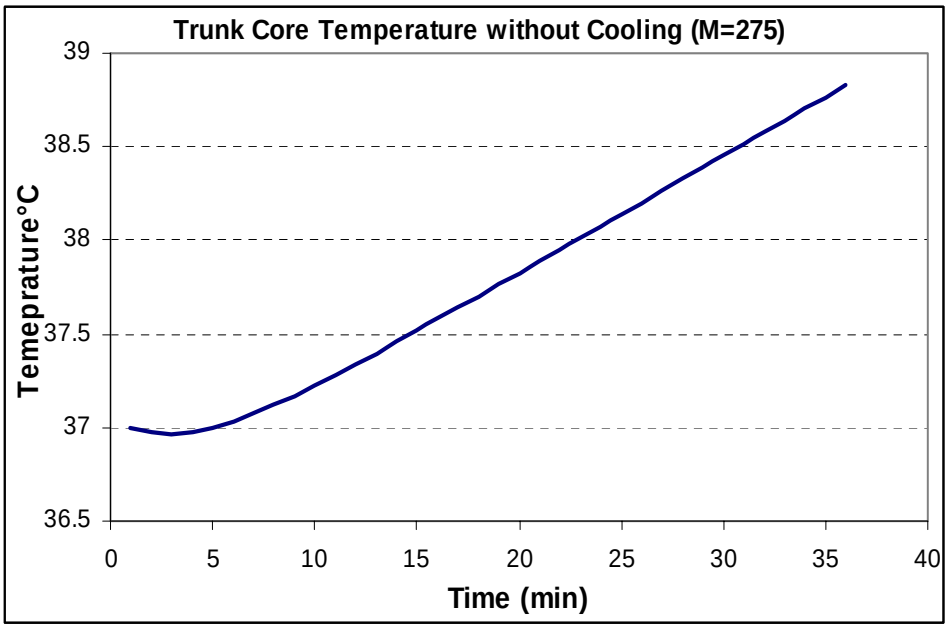

Figure 5.17 Trunk Core Temperature

Case 2: Water Cooling System (hot condition Ls253 8S 75W 13 hours-17 hours)

This case is based on the exact same conditions with that of case 1 except the introduction of water cooling system. The simulation results are shown in Figure 5.18, Figure 5.19 and Figure 5.20. The trunk core temperature is kept below 38.5°C during the 4 hour working period (13 hours-17 hours). The inlet temperature of cooling water is 20°C. Figure 5.20 shows the heat removed from human body by water cooling system

together with the inlet and outlet temperature of cooling water. The heat removed by cooling water is calculated by the difference between inlet and outlet temperature of cooling water. Figure 5.19 shows the total heat leak, which is the heat lost to the environment through the insulation and suit enclosure. Heat leak includes three terms: absorbed thermal radiation, emitted radiation from the suit surface and convective heat lost to environment gas. Heat leak is very useful in estimating the required cooling needs. The outside temperature of space suit is showed in Figure 5.21.

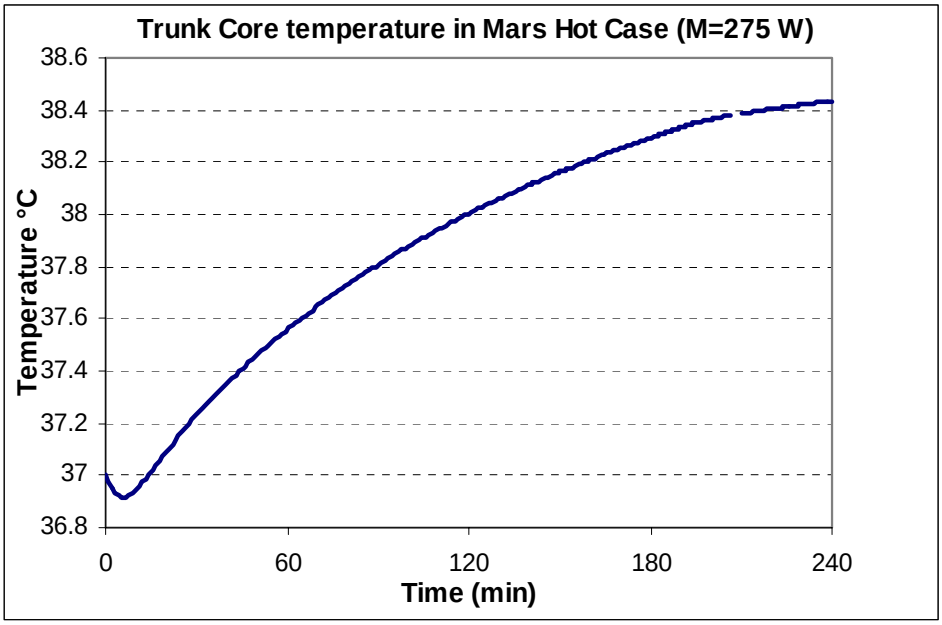

Figure 5.18 Trunk Core Temperature with Water Cooling System

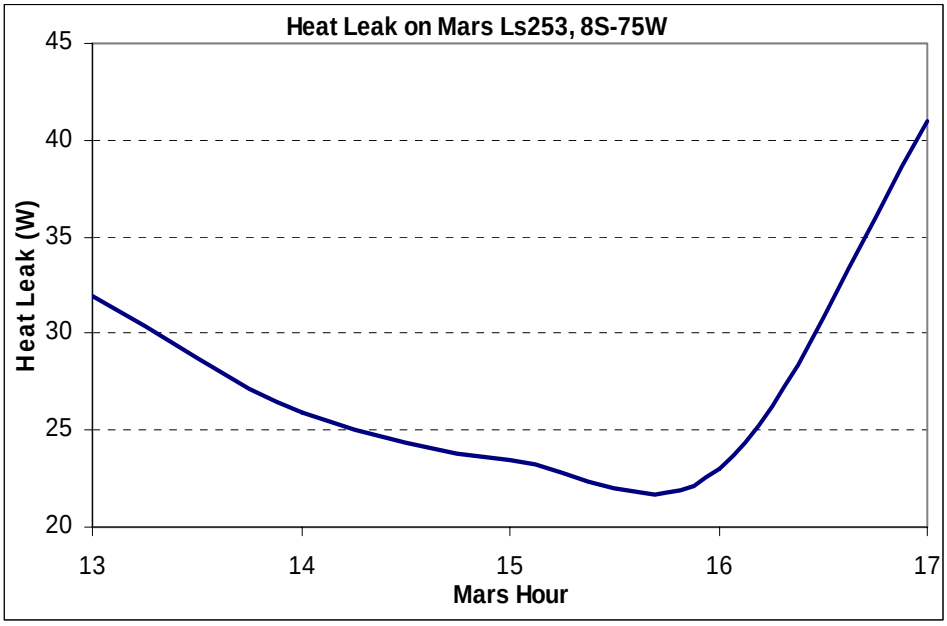

Figure 5.19 Heat Leak from Human Body to Environment (Hot Case)

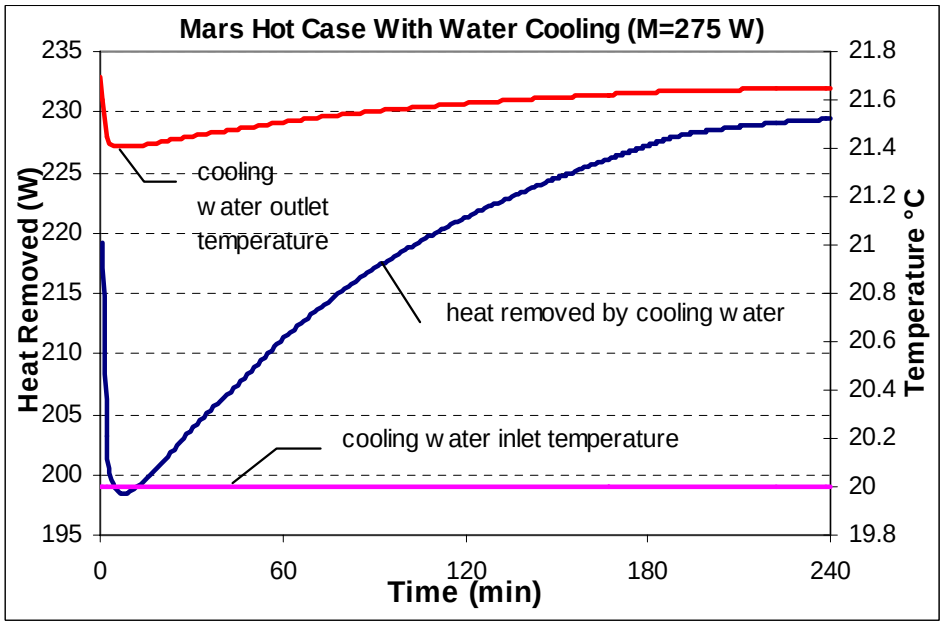

Figure 5.20 Heat Removal , Inlet and Outlet Cooling Water Temperature

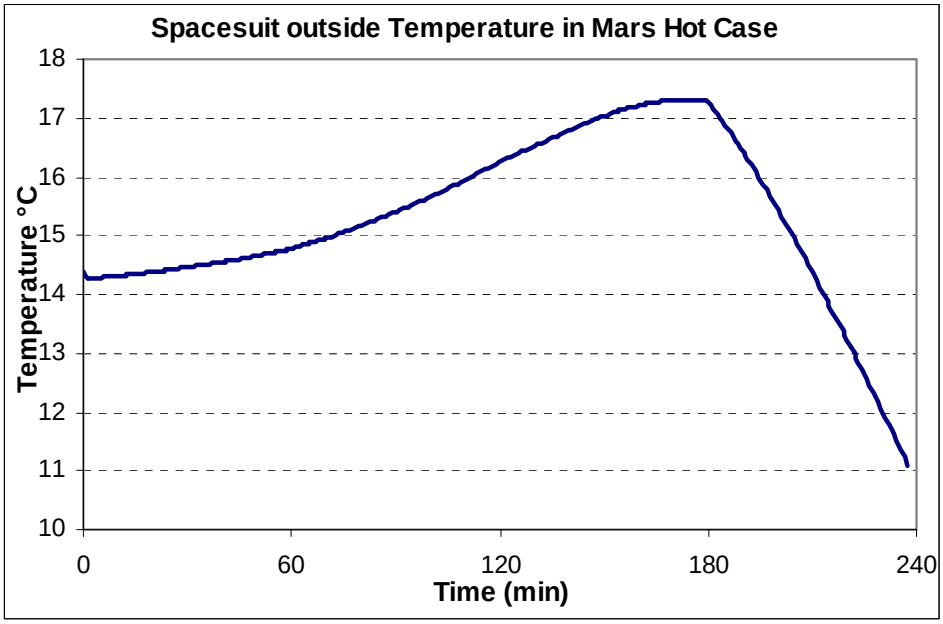

Figure 5.21 Outside Temperature of Spacesuit (Hot Case)

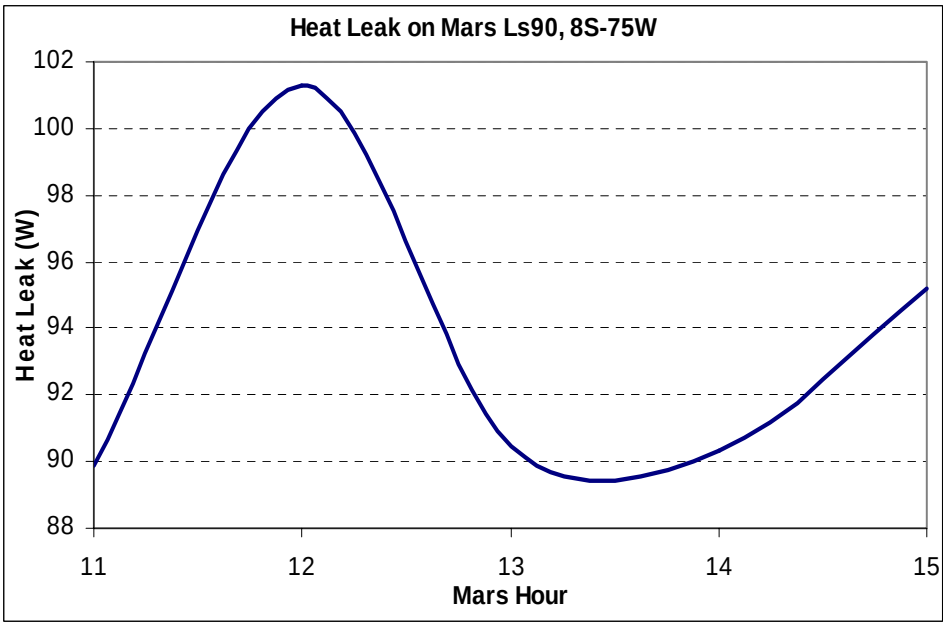

Figure 5.22 Heat Leak from Human Body to Environment (Nominal Cold

Case 3: Water Cooling System (nominal cold condition Ls90 8S 75W 11 hours-15 hours)

Case 3 is similar with case 2 except that case 3 has a different environment condition; Figure 5.22 shows the heat leak for nominal cold case. The outside temperature of space suit is showed in Figure 5.23.

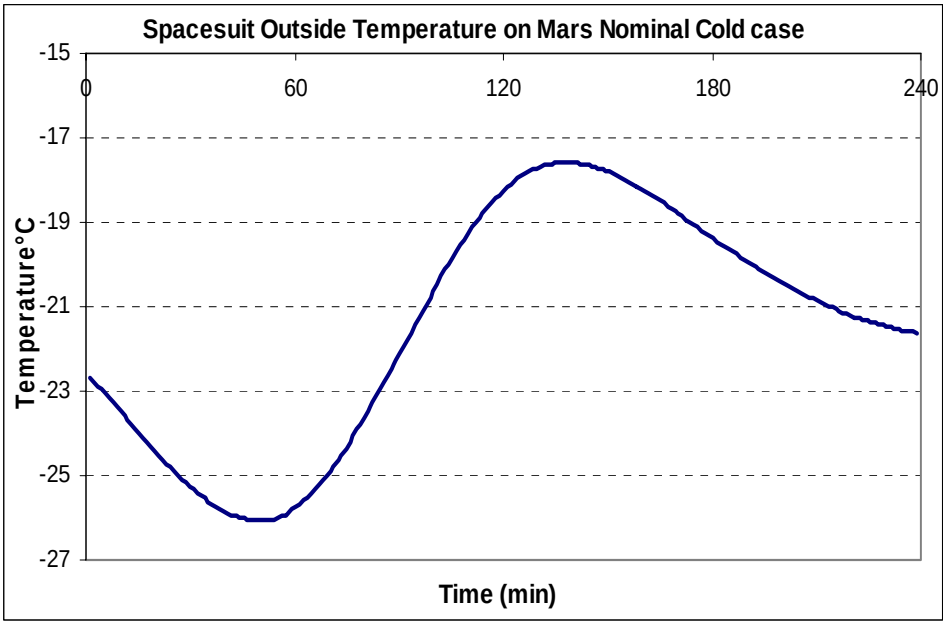

Figure 5.23 Outside Temperature of Spacesuit (Nominal Cold Case)

Figure 5.24 shows the required heat removal from human body on mars hot case from time 6 hour to 19 hour. The above data provides useful information to design heat cooling system. Figure 5.25 shows a simplified schematic of the current system with the EVA crewmember in the loop. Heat rejection takes place using a sublimator that carries a logistics penalty (loss of 7 lb of water per EVA per crewperson) and can only operate in a vacuum. As pointed out earlier, the sublimator in the cooling loop should be

avoided for Mars applications as water may have to be conserved on Mars. The alternative would be a radiator that takes advantage of typical low radiation sink temperatures, such as the one depicted in Figure 5.26. However, such arrangement does not always work as an excessive radiator surface area may be needed.

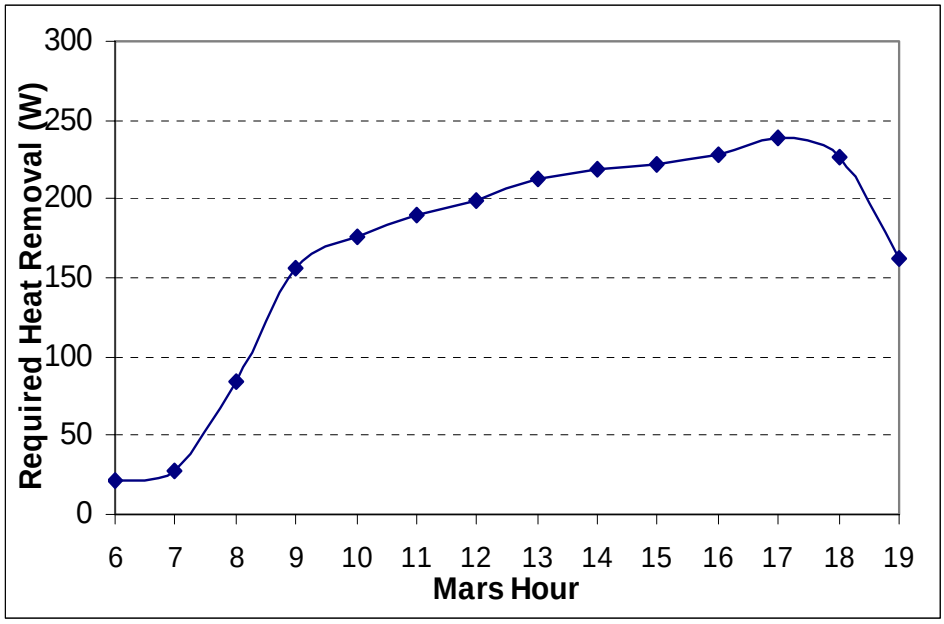

Figure 5.24 Required Heat Removal for Hot Case on Mars

Figure 5.27 shows simplified flow schematic shuttle EMU with MVCC. Sublimator is replaced by a miniature vapor compression system to eliminate water loss. The radiator size is reduced due to high radiation temperature. Our calculations shows that personal cooling system with MVCC can provide adequate heat removal for nominal cold case and provide extended exposure time for hot case on Mars.

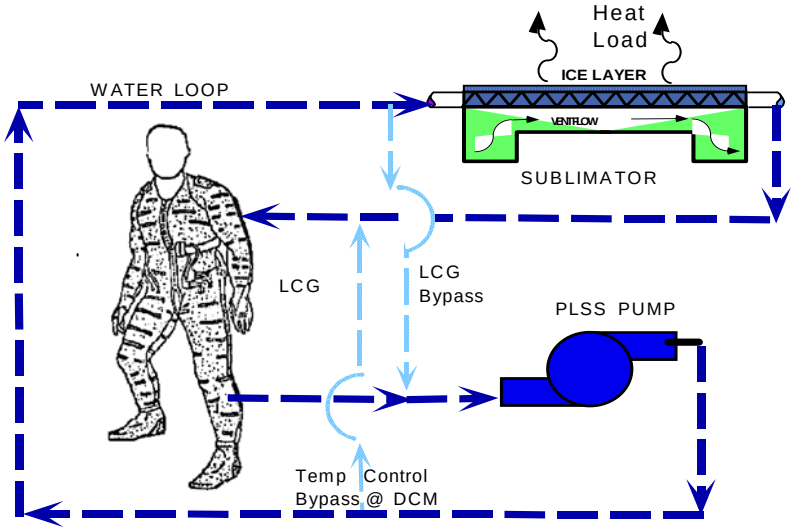

Figure 5.25. Simplified Flow Schematic shuttle EMU Water Loop

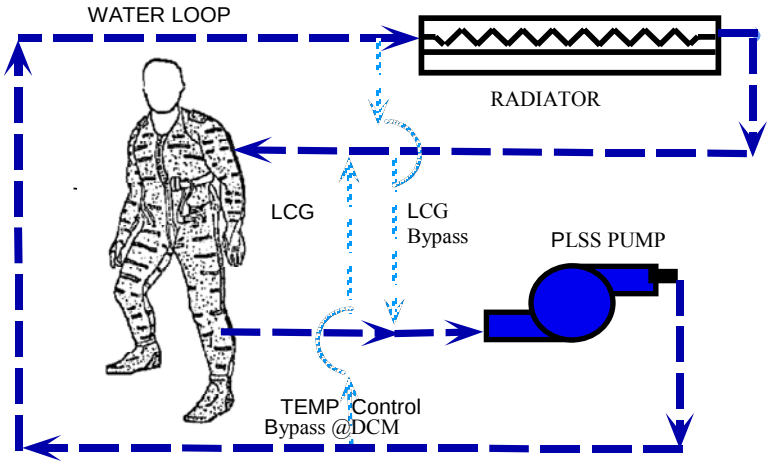

Figure 5.26 Simplified Flow Schematic Shuttle EMU with Radiator

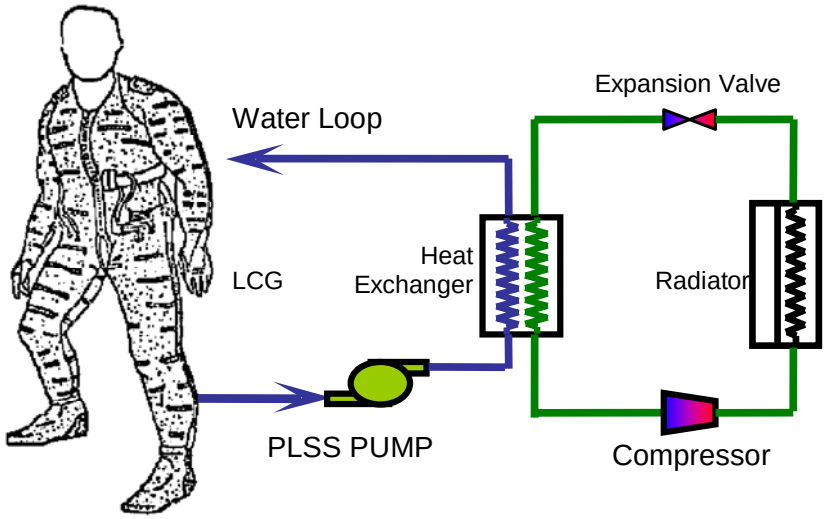

Figure 5.27 Simplified Flow Schematic Shuttle EMU with MVCC

CHAPTER 6 SUMMARY AND CONCLUSIONS

Summary

This dissertation deals with heat stress prediction for persons wearing PPE with various cooling systems. Individuals show large variations in the reactions to heat exposure with different cooling system. A thermal model is developed to carry out the predictions. Such model will improve risk assessment and it is especially useful to use the predictions to select and design cooling systems.

Chapter 1 first introduces simple information of 4 levels of personal protective equipment. This dissertation mainly concentrates on level A PPE since the high possibility of heat stress due to its high heat resistance and vapor impermeability. Second, Chapter 1 explains how the human body regulates its temperature when it is being exposed to varying environments. Third, the mechanisms of heat transfer from body to ambient are introduced. Finally, several different cooling systems are introduced and the comparisons among the different cooling systems are presented in Chapter 1.

Chapter 2 reviews the literature on thermoregulatory models and clothing models. The detailed descriptions of thermal model are presented in Chapter 3. Individual characteristics, such as height, weight and initial trunk core temperature, have

significant effects on human thermal response. These characteristics are incorporated into the original thermoregulatory model to provide better predictions. Water cooling model, air cooling and ice cooling model are presented. Cooling models are integrated with thermoregulatory model and carried out by using control volume method. A water cooling lumped model is also presented in this chapter.

Chapter 4 presents detailed USF experiment descriptions, which include climatic chamber conditions, cooling system used, subjects' detailed information and experiments measurement. The thermal model is validated by comparing simulation results with USF experiment data in this chapter. The limitation of the thermal model is discussed.

In Chapter 5, the predictioned results of thermal model are compared with that from lumped model. Parametric studies are carried out for both water cooling and air cooling. A typical extra-vehicular activity (EVA) on Mars is simulated by the thermal model. The results provide very useful information on designing cooling system.

Conclusions

From the studies presented in this dissertation, the thermal model has proved to be valuable tool for predicting human thermal response and the effects of cooling system

on human body. The model is effective for impermeable PPE and any permeable clothing in varying environment conditions. The discrepancy between simulations results and experimental data mainly happens in the first several minutes when the cooling system is turned on or there is a metabolic rate jump. It is concluded that the discrepancy results from the inappropriate assumptions of thermoregulatory model. To further improve the predictions, a more complex thermoregulatory model is needed by taking account of cardiovascular and the respiratory system effects.

Compared with lumped model, the thermal model could provide much better prediction and this thermal model can be used to estimate cooling needs, choose proper capacity of cooling system and predict working time permitted. For water cooling, the parametric studies show that lower metabolic rate, cooling water inlet temperature and liner resistance could increase the maximum exposure time dramatically, however, cooling water flow rate and PPE thermal resistance do not have much impact on the maximum exposure time. For air cooling the parametric studies show that cooling air flow rate, inlet temperature and liner resistance have great impact on the maximum exposure time. The relative humidity of cooling air does not have much impact on the maximum exposure time for low metabolic rate cases, however it does make difference if the metabolic rate is high.

;

APPENDIX A PARAMETERS FOR THERMOREGULATORY MODEL

Table A1 Heat Capacity for Each Body Part of a Standard Man

(Stolwijk and Hardy, 1977) W h/.°C

Body Parts	Core	Muscle	Fat	Skin
Head	2.57	0.39	0.26	0.28
Trunk	11.44	18.80	4.94	1.41
Arms	1.63	3.54	0.67	0.5
Hands	0.16	0.07	0.10	0.2
Legs	4.94	10.19	1.66	1.25
Feet	0.27	0.07	0.15	0.26
Blood	2.60			

Table A2 Density for Each Body Part of a Standard Man

(Stolwijk and Hardy, 1977) J/kg.°C

Body Parts	Core	Muscle	Fat	Skin
Head	1000	1000	1000	1000
Trunk	829.7003	1000	1000	1000
Arms	1004.464	1000	1000	1000
Hands	1000	1000	1000	1000
Legs	1004.342	1000	1000	1000
Feet	1000	875	1000	1000
Blood	1000			

Table A3 Average Thermal Conductance for Each Compartment of a Standard Man

(Stolwijk and Hardy, 1977) W/(cm. °C) $\times 10^4$

	Core	Muscle	Fat	Skin
Head	41.8	41.8	33.4	33.4
Trunk	41.8	41.8	33.4	33.4
Arms	41.8	41.8	33.4	33.4
Hands	41.8	41.8	33.4	33.4
Legs	41.8	41.8	33.4	33.4
Feet	41.8	41.8	33.4	33.4

Table A4 Heat Transfer Coefficient for Each Body Part of a Standard Man

(Stolwijk and Hardy, 1977) W/(m^2°C)

Head		Trunk		Arms		Hands		Legs		Feet	
Rad.	Conv.	Rad.	Conv.	Rad.	Conv.	Rad.	Conv.	Rad.	Conv.	Rad.	Conv.
4.8	3.0	4.8	2.1	4.2	2.1	3.6	4.0	4.2	2.1	4.0	4.0

Note: Radiation heat transfer is ignored inside PPE.

Table A5 Set Point Values and Initial Condition Temperatures of a Standard Man

(Stolwijk and Hardy, 1977) (°C)

	Core	Muscle	Fat	Skin	Central Blood
Head	36.96	35.07	34.81	34.58	36.71
Trunk	36.89	36.28	34.53	33.62	
Arms	35.53	34.12	33.59	33.25	
Hands	35.41	35.38	35.3	35.22	
Legs	35.81	35.30	35.31	34.10	
Feet	35.14	35.03	35.11	35.04	

Table A6 Estimated Basal Heat Production for Each Compartment of a Standard Man

(Stolwijk and Hardy, 1977) (W)

	Core	Muscle	Fat	Skin
Head	14.95	0.12	0.13	0.10
Trunk	52.63	5.81	2.49	0.47
Arms	0.82	1.11	0.21	0.15
Hands	0.09	0.23	0.04	0.06
Legs	2.59	3.32	0.50	0.37
Feet	0.15	0.02	0.05	0.08

Table A7 Estimated Basal Blood Flow for Each Compartment of a Standard Man

(Stolwijk and Hardy, 1977) (l/h)

	Core	Muscle	Fat	Skin
Head	45.00	0.12	0.13	1.44
Trunk	210.00	6.00	2.56	2.10
Arms	0.84	1.14	0.20	0.50
Hands	0.10	0.24	0.04	2.00
Legs	2.69	3.43	0.52	2.85
Feet	0.16	0.02	0.05	3.00

Table A8 Estimated Basal Evaporative Heat for Each Compartment of a Standard Man

(Stolwijk and Hardy, 1977) (l/h)

	Core	Muscle	Fat	Skin
Head	0	0	0	0.81
Trunk	10.45	0	0	3.78
Arms	0	0	0	1.4
Hands	0	0	0	0.52
Legs	0	0	0	3.32
Feet	0	0	0	0.72

Table A9 Estimated Volume for Each Compartment of a Standard Man (cm^3)

(Stolwijk and Hardy, 1977) (cm^3)

	Core	Muscle	Fat	Skin	Central Blood
Head	3010	370	370	270	2500
Trunk	14680	17900	7070	1350	
Arms	2240	3370	970	480	
Hands	260	70	150	190	
Legs	6910	10190	2380	1200	
Feet	430	80	220	240	

Table A2 Estimated Raius and Length for Each Compartment of a Standard Man

(Stolwijk and Hardy, 1977) (cm)

	Length (cm)	Diameter (cm)			
		Core	Muscle	Fat	Skin
Head		8.98	9.32	9.65	9.88
Trunk	60	8.75	13.15	14.40	14.70
Arms	112	2.83	4.48	4.85	5.02
Hands	96	0.93	1.04	1.27	1.49
Legs	160	3.71	5.85	6.23	6.42
Feet	125	1.06	1.14	1.36	1.57

Table A3 Surface Area and Estimates of Distribution of Sensory Input and Effector Output Over the Various Skin Areas for Each Body Part of a Standard Man
(Stolwijk and Hardy, 1977)

	Surface Areas		SKINR	SKINS	SKINV	SKINC
	m^2	%				
Head	0.1326	7.00	0.21	0.081	0.132	0.05
Trunk	0.6804	36.02	0.42	0.481	0.322	0.15
Arms	0.2536	13.41	0.10	0.154	0.095	0.05
Hands	0.0946	5.00	0.04	0.031	0.121	0.35
Legs	0.5966	31.72	0.20	0.218	0.230	0.05
Feet	0.1299	6.85	0.03	0.035	0.10	0.35
Total	1.8877	100.00	1.00	1.00	1.00	1.00

Table A4 Estimates of Distribution of Heat Production in Muscle Compartments for Each Body Part of a Standard Man
(Stolwijk and Hardy, 1977)

	% of Total Muscle Mass	WORKM	CHILM
Head	2.323		0.02
Trunk	54.790	0.30	0.85
Arms	10.525	0.08	0.05
Hands	0.233	0.01	0.00
Legs	31.897	0.60	0.07
Feet	0.233	0.01	0.00

Table A5 Weight for Each Body Part of a Standard Man

(Stolwijk and Hardy, 1977) (kg)

Body Parts	Total		Core			Muscle	Fat	Skin
	kg	%	Skeleton	Viscera	Total			
Head	4.02	5.4	1.22	1.79	3.01	0.37	0.37	0.27
Trunk	38.50	51.7	2.83	9.35	12.18	17.90	7.07	1.35
Arms	7.06	9.5	1.51	0.74	2.25	3.37	0.97	0.48
Hands	0.67	0.9	0.23	0.03	0.26	0.07	0.15	0.19
Legs	20.68	27.8	5.02	1.92	6.94	10.19	2.38	1.20
Feet	0.97	1.3	0.37	0.06	0.43	0.07	0.22	0.24
Blood	2.5	3.4		2.50	2.50			
Total	74.4	100.00	11.18	16.39	27.57	31.97	11.16	3.73

Table A6 Thermal Conductance Between Compartments

(Stolwijk and Hardy, 1977) W/°C

	Core	Muscle	Fat	Skin
Head	1.61	13.25	16.1	
Trunk	1.59	5.53	23.08	
Arms	1.4	10.3	30.5	
Hands	6.4	11.2	11.5	
Legs	10.5	14.4	74.5	
Feet	16.3	20.6	16.4	

APPENDIX B METABOLIC RATE FOR TYPICAL ACTIVITIES

Table B7 Metabolic Rate and Mechanical Efficiency at Different Typical Activities

(Fanger, 1970)

Activities		**Metabolic rate M/A_{Du} kcal/hr m^2**	**Mechanical Efficiency η**
Sleep		35	0
Reclining		40	0
Seated, quiet		50	0
Standing, relaxed		60	0
walking			
On the level	km/hr		
	3.2	100	0
	4.0	120	0
	4.8	130	0
	5.6	160	0
	6.4	190	0
	8.0	290	0
Up a grade			
% Grade	km/hr		
5%	1.6	120	0.07
5%	3.2	150	0.10
5%	4.8	200	0.11
5%	6.4	305	0.10
15%	1.6	145	0.15
15%	3.2	230	0.19
15%	4.8	35	0.19
25%	1.6	180	0.20
25%	3.2	335	0.21
Miscellaneous occupations			
Bakery (e.g. cleaning tins, packing boxes)		70-100	0-0.1

Brewery (e.g. filling bottles, loading beer boxes onto belt)	60-120	0-0.2
Activities	**Metabolic rate M/A_{Du} kcal/hr m^2**	**Mechanical Efficiency η**
carpentry		
Machine sawing	90	0
Sawing by hand	200-240	0.1-0.2
Planning by hand	280-320	0.1-0.2
Foundry work		
Fettling (pneumatic hammer)	160	0.1-0.2
Tipping the moulds	200	0.1-0.2
Roughing (i.e. carrying 60kg).	270	0.1-0.2
Tending the furnace	340	0.1-0.2
Slag removal	380	0.1-0.2
Garage work (e.g. replacing tyres, raising cars by jack))	110-150	0-0.1
Laboratory work		
Examine slides	70	0
General laboratory work	80	0
Setting up apparatus	110	0
locksmith	110	0-0.1
Machine work		
Light (e.g. electrical industry)	100-120	0-0.1
Machine fitter	140	0-0.1
Heavy (e.g. paint industry)	200	0-0.1
Manufacture of tins (e.g. filling, labeling and dispatch)	100-200	0-0.1
Seated, heavy limb movements(e.g. metal worker)	110	0-0.2
Shoemaker	100	0-0.1
Shop assistant	100	0-0.1
Teacher	80	0
Watch repairer	55	0
Vehicle driving		
Car(light traffic)	50	0
Car (heavy traffic)	100	0
Heavy vehicle (e.g. power truck)	160	0-0.1

Night flying		60	0
Instrument landing		90	0
Combat flying		120	0
Activities		**Metabolic rate M/A_{Du} kcal/hr m^2**	**Mechanical Efficiency η**
Heavy work			
Pushing wheelbarrow (57kg at 4.5km/hr)		125	0.2
Handling 50kg bags		200	0.2
Pick & shovel work		200-240	0.1-0.2
Digging trenches		300	0.2
Domestic work			
House cleaning		100-170	0-0.1
Cooking		80-100	0
Washing dishes, standing		80	0
Washing by hand and ironing		100-180	0-0.1
Shaving, washing and dressing		85	0
shopping		80	0
Office work	wpm		
Typing (electrical)	30	45	0
	40	50	0
Typing 9mechanical)	30	55	0
	40	60	0
Adding machine		60	0
Miscellaneous office work (e.g. filing, checking ledgers)		50-60	0
draughtsman		60	0
Leisure activities			
Gymnastics		150-200	0-0.1
Dancing		120-220	0
Tennis		230	0-0.1
Fencing		350	0

Squash	360	0-0.1
basketball	380	0-0.1
wrestling	435	0-0.1

APPENDIX C THERMAL RESISTANCE FOR TYPICAL CLOTHING

Table C8 Overall Thermal Resistance Values for Typical Clothing Ensembles

(Fanger, 1970; SCENHRS1, 1997)

Clothing Ensemble	clo	Clothing Ensemble	clo
Nude	0	Shorts	0.1
Typical Tropical Clothing Ensemble: Shorts, open-neck shirt with short sleeves, light socks and sandals	0.3-0.4	Apollo Constant Wear Garment (astronauts): Light cotton undergarment with short sleeves and ankle length legs, cotton socks	0.35
Light Summer Clothing: Long light-weight-trousers, open neck shirt with short sleeves	0.5	Light Working Ensemble: Athletic shorts, woolen socks, cotton work shirt(open-neck), and work trousers, shirt trail out(208)	0.6
U>S. Army “Fatigues”, Man’s: Light-weight underwear, cotton shirt and trousers, cushion sole socks and combat boots	0.7	Heavy Wool Pile Ensemble: (Polar weather suit)	3-4
Typical Business Suit	1.0	Typical Business Suit+ Cotton Coat	1.5
U.S. Army Standard Cold-wet Uniform: Cotton-wool undershirt and drawers, wool and nylon flannel shirt, wind resistant, water repellent trousers and field coat, cloth mohair and wool coat liner and wool socks	1.5-2.0	Combat Tropical Uniform: Same general components as U.S. Army fatigues but with shirt and trousers of cloth, wind resistant, poplin	0.8
Us Army Woodland Battledress Overgarment (BDO), Underwear, Mask, Gloves, Detached Impermeable Hood.	1.7	Us Army Woodland Battledress Overgarment (BDO) + Uniform, Mask, Gloves, Impermeable Hood.	2.1
US army woodland temperate BDU + ECWCS Parka with Field Coat Liner	1.6	Us army aircrew uniform integrated Battlefield (AUIB) + US army chemical protective undergarment (CPU), Mask, gloves, impermeable Hood	1.6
US air force Groundcrew coveralls (CWU/77P) + underwear, mask, gloves, impermeable hood	1.2	US army woodland temperate BDU + ECWCS Parka	1.4
Canadian Threat Oriented Protective Posture (TOPP-High) using: Canadian coverall + Canadian combat clothing lightweight MK 2 Coat + trousers, mask, gloves, hood	1.9	United Kingdom MARK IV, CP overgarment + underwear, Mask, gloves, Attached hood	1.8
United Kingdom MARK IV + US battledress Uniform, mask, gloves, attached hood	1.9	United Kingdom MARK IV + UK army fatigues, mask, gloves, attached hood	1.8
United Kingdom MARK IV + UK army fatigues (flame resistant), UK navy coverall (Flame resistant), mask, gloves, attached hood	2.1	Canadian Threat Oriented Protective Posture using: Canadian coverall Alone + CW mask, gloves, attached hood	1.5

Note: clo = $0.155 m^2$ °C/W

APPENDIX D PHYSIOLOGICAL DATA OF SUBJECTS IN USF EXPERIMENT

Table D9. List of Subjects' Weight, Height, Gender and Age

Subject	Gender	Height (cm)	Weight (kg)	Age (yr)
A	M	180	95	44
B	M	193	86	23
C	F	172	53	22
D	M	180	76	23
E	F	165	60	35
F	F	163	53	35
G	M	163	57	43
H	M	183	90	35
I	M	173	73	6
J	M	137	70	27
K	M	185	83	39

LIST OF REFERENCES

ASHRAE, 1977, *Physiological Principles, Comfort and Health*, Handbook of Fundamentals, American Society for Heating, Refrigeration, and Air-Conditioning Engineers, Atlanta, pp. 8.1-8.36

ASHRAE Standard 55, 1992, *Thermal Environmental Conditions for Human Occupancy*, American Society for Heating Refrigerating and Air-conditioning Engineers, Atlanta.

Breckenridge, J. R., 1977, *Effects of Body Motion on Convective and Evaporative Heat Exchanges through Various Designs of Clothing*. Clothing Comfort, Ann Arbor Science, Ann Arbor. pp. 153-166.

Chato, J. C., 1980, *Heat Transfer to Blood Vessels*, ASME Journal of Biomechanical Engineering 102: 110-118

Chen, M. M. and K. R. Homes, 1980, *Microvascular Contribution in Tissue Heat Transfer*, NYAS (Annals of the New York Academy of Science) 335:137-150.

Dubois D. and Dubois E.F., 1916, *A Formula to Estimate the Approximate Surface Area if Height and Weight are Known*, Archives of Internal Medicine 17: pp. 863–871.

Fanger, P.O., 1970, *Thermal Comfort, Analysis and Applications in Environmental Engineering*. McGraw-Hill Book Company.

Fernandes, F. I., 2002, *Heat Stress and Personal Cooling Garments,* Thesis, University of South Florida.

Gagge, A.P. and Nishi, Y., 1977, *Heat Exchange between Human Skin Surface and Thermal Environment*, Handbook of Physiology, Chapter 5: pp.69-92.

Gnielinski, V., 1975, *Berechnung mittlerer Wärme- und Stoffübergangskoeffizienten an Laminar und Turbulent überströmten Einzelkörpern mit Hilfe Einer Einheitlichen Gleichung*", Forschung im Ingenieurwesen 41: pp. 145-153.

Kerslake, D. M., 1972, *the Stress of Hot Environment*, Cambridge: Cambridge University Press.

Iovine, J.V. and Horton, R.D., 1999, *Preliminary Design Review (PDR) - Advanced Technology Spacesuit Thermal Module Thermal Systems Analysis*, Lockheed Martin Space Operations, 1999.

McIntyre DA, 1980, *Indoor Climate*. London: Applied Science

Parsons, K.C., 1993, *Human Thermal Environments*, Tayler&Francis

Stolwijk, J.A.J. and Hardy, J.D., 1966, *Temperature Regulation in Man - a Theoretical Study*. Pflugers Archiv 291:129-162.

Stolwijk, J.A.J. and Hardy, J.D., 1977, *Control of Body Temperature*, in Handbook of Physiology, Chapter 4, pp45-68

Werner J, 1989, *Thermoregulatory models. Recent research, current applications and future development*. Scand. J Work Environ Health 15:34-46

Werner J, Webb P, 1993, *A six-cylinder model of human thermoregulation for general use on personal computers*. The annals of physiological anthropology 12: 123-134

Wissler EH, 1964, *A Mathematical Model of the Human Thermal System*. Bulletin of mathematical biophysics 26:147-167.

Wissler EH, 1982, *An Evaluation of Human Thermal Models*. Report on a workshop, University of Austin (Tx) dec 13-15

Wissler, E. H., 1985, *Mathematical Simulation of Human Thermal Behavior Using Whole-Body Models*, Heat Transfer in Medicine and biology, Volume I, Chapter 13

Yin, Y., 2002, *Liquid Cooling Garment for Personal Protective Ensemble--- Modeling and Simulation*, MS thesis, University of Central Florida